Millennial hydrological variability in the continental northern Neotropics during MIS3-2 (59-15 cal ka BP) inferred from sediments of Lake Petén Itzá, Guatemala

Rodrigo Martínez-Abarca[1*], Michelle Abstein[1], Frederik Schenk[2,3], David Hodell[4], Philipp Hoelzmann[5], ~~David Hodell[3]~~, Mark Brenner[6], Steffen Kutterolf[7], Sergio Cohuo[8], Laura Macario-González[9], Mona Stockhecke[10], Jason Curtis[6], Flavio S. Anselmetti[11], Daniel Ariztegui[12], Thomas Guilderson[13,14], Alexander Correa-Metrio[15,16], ~~Frederik Schenk[15,16]~~, Thorsten Bauersachs[17], Liseth Pérez[1], and Antje Schwalb[1]

[1]Institut für Geosysteme und Bioindikation, Technische Universität Braunschweig, Braunschweig, 38106, Germany
[2]Department of Geological Sciences and Bolin Centre for Climate Research, Stockholm University, Stockholm, 10691, Sweden
[3]Department of Geosciences and Geography, University of Helsinki, Helsinki, FI-00014, Finland
[4]Godwin Laboratory for Palaeoclimate Research, Department of Earth Sciences, University of Cambridge, Cambridge, CB2 3EQ, UK
[5]Institut für Geographische Wissenschaften, Physische Geographie, Freie Universität Berlin, Berlin, 12249, Germany
~~[3]Godwin Laboratory for Palaeoclimate Research, Department of Earth Sciences, University of Cambridge, Cambridge, CB2 3EQ, UK~~
[6]Department of Geological Sciences and Land Use and Environmental Change Institute, University of Florida, Florida, 32611, USA
[7]GEOMAR Helmholtz Centre for Ocean Research Kiel, Kiel, 24148, Germany
[8]Tecnológico Nacional de México/I.T. de Chetumal, Chetumal, 77013, Mexico
[9]Tecnológico Nacional de México/I.T. de la Zona Maya, Quintana Roo, 77013, Mexico
[10]Large Lakes Observatory (LLO), University of Minnesota-Duluth, Minnesota, 55812, USA
[11]Institute of Geological Sciences and Oeschger Centre for Climate Change Research, University of Bern, Bern, 3012, Switzerland
[12]Department of Earth Sciences, University of Geneva, Geneva, 1205, Switzerland
[13]Center for Accelerator Mass Spectrometry, Lawrence Livermore National Laboratory, California, 94550, USA
[14]Ocean Sciences Department, University of California–Santa Cruz, California, 95064, USA
[15]Instituto de Geología, Universidad Nacional Autónoma de México, Mexico City, 04510, Mexico
[16]Centro de Geociencias, Universidad Nacional Autónoma de México, Juriquilla, 76230, Mexico
~~[15]Department of Geological Sciences and Bolin Centre for Climate Research, Stockholm University, Stockholm, 11418, Sweden~~
~~[16]Department of Geosciences and Geography, University of Helsinki, Helsinki, FI-00014, Finland~~
[17]Institute of ~~Geosciences, Organic Geochemistry Group, Christian-Albrechts-University, Kiel, 24118, Germany~~ Earth Sciences, Heidelberg University, Heidelberg, 69120, Germany.

Correspondence to: Rodrigo Martínez-Abarca (j.martinez-abarca@tu-bs.de)

Abstract. Lake Petén Itzá (Guatemala) possesses one of the longest lacustrine sediment records in the northern Neotropics, which enabled study of paleo-climate variability in the region during the last ~400,000 years. We used ~~We inferred hydrological changes in Lake Petén Itzá (Guatemala) during Marine Isotope Stages (MIS) 3-2 using~~ geochemical (Ti, Ca/(Ti~~+Al~~+Fe) ~~ratio~~ and Mn/Fe) and mineralogical (carbonates, gypsum, quartz, clay) data from sediment core PI-2 to infer past ~~reconstruct~~ changes in runoff, lake evaporation, organic matter sources and ~~potential oxic/anoxic~~redox conditions in the water column, caused by hydrological changes in the northern Neotropics during Marine Isotope Stages (MIS) 3-2. ~~associated with variations in water-level during the last ~59 cal ka BP. Early~~ From 57 to 39 cal ka BP climate conditions were ~~MIS3 (57.0-52.5 cal ka BP) was dominated by~~ relatively wet and the lake

Con formato: Sin Superíndice / Subíndice
Con formato: Sin Superíndice / Subíndice
Con formato: Inglés (Estados Unidos)
Con formato: Inglés (Estados Unidos)
Con formato: Color de fuente: Automático
Código de campo cambiado
Con formato: Color de fuente: Automático
Con formato: Color de fuente: Automático
Con formato: Color de fuente: Automático

was marked by ~~conditions,~~ higher ~~lake~~ primary productivity ~~and~~ anoxic bottom waters. This wet environment is interrupted for two periods of possible low water-level at 52 and 46 cal ka BP when our data suggest higher evaporation, high terrestrial organic matter input and persistent oxic conditions.~~, which persisted into the subsequent interval (52.5-39.0 cal ka BP), except for two periods of possible low water-level at 52 and 46 cal ka BP when our data suggest higher evaporation, high terrestrial organic matter input and persistent oxic conditions.~~ Between 39 and 23 cal ka BP, ~~Towards the end of MIS3 and start of MIS2 (39.0-23.0 cal ka BP), lake~~ evaporation and ~~-~~input of terrestrial organic matter increased considerably, lake level declined and lake bottom waters generally became oxic. ~~as did inputs of terrestrial organic matter, and waters became more oxic as water levels dropped and the site moved from the hypolimnion to the epilimnion. These~~ These ~~conditions reversed~~conditions reversed during the Last Glacial Maximum (23.0-18.0 cal ka BP) when runoff and lake productivity increased and ~~waters again became anoxic as a result of~~ rising lake level caused bottom waters to again become anoxic~~rising water levels~~. Comparison of our hydrologic proxy data with sea surface temperature anomalies between the eastern Pacific and the Caribbean suggest that changes in the intensity of the Caribbean Low-Level Jet (CLLJ) may have influenced long-term changes in runoff during MIS3-2. A higher intensity of the CLLJ during the onset of MIS3 and the LGM might have led to greater runoff into the lake, whereas the MIS3-2 transition experienced a weaker CLLJ and consequently less runoff. A ~~Refini~~refined~~ng~~, high resolution ~~the~~ age-depth model for the ~~Site~~ PI-2 sediment core enabled us ~~also allowed~~ to identify~~the correlation to~~ millennial-scale ~~-~~Greenland Interstadials (GI14-2), Greenland Stadials (GS14-2) and Heinrich Stadials (HS5-1). In general, HS and GS were characterized by ~~increases in Ca/Ti+Al+Fe ratios and gypsum content generally indicative of~~ drier conditions. In contrast to GS and HS, GI were characterized by greater runoff and overall wetter conditions, with the most pronounced GI peaks between 40 and 30 cal ka BP. Whereas GS~~13,~~ 9, 8, 7 and ~~5~~6 began with abrupt increases in evaporation and ended with gradual increases in humidity, GS 11 and 10 show reversed patterns. The Lake Petén Itzá paleohydrology record, along with other regional paleoclimate records led us to conclude that shifts in the position of the Intertropical Convergence Zone (ITCZ) altered moisture delivery to the lake on millennial timescales. During GS and HS, high evaporation from Petén Itzá (dry climate conditions) was associated with a more southerly position of the ITCZ, whereas wetter GI prevailed during a more northerly ITCZ position. Whereas abrupt millennial-scale shifts in ITCZ and hydroclimate between GS/HS and GI can be linked to instabilities in the Atlantic Meridional Overturning Circulation (AMOC), longer-term changes were additionally influenced by changes in atmospheric convection linked to modulations of the CLLJ in response to ΔSST between the equatorial Pacific and tropical Atlantic.

~~showed the driest conditions associated with the contemporaneous establishment of HS5-3, respectively. In contrast, GI show high Ti values which suggests relatively greater runoff and overall wetter conditions compared with GS and HS, with the most marked GI peaks between 40 and 30 cal ka BP. This runoff variability is in accord with shifts in the average position of the Intertropical Convergence Zone and strength of the Atlantic Meridional Oceanic Circulation during the Late Pleistocene.~~

1 Introduction

The last glacial period (115-11.7 cal ka BP) ~~in the high latitudes of the northern hemisphere~~ was marked by strong millennial-scale climate variability in the high-latitude Northern Hemisphere. Marine Isotope Stages (MIS) 3 (57-29 cal ka BP) and the last deglaciation (19-1~~1~~0.57 cal ka BP) were ~~characterized~~ dominated by abrupt climate events (e.g.

Con formato: Color de fuente: Automático

Con formato: Color de fuente: Automático

Con formato: Color de fuente: Automático

Con formato: Color de fuente: Automático

Con formato: Color de fuente: Automático

Heinrich, 1988; Lisiecki and Stern, 2016; Bradley and Diaz, 2021). ~~-~~In the Greenland ice core, these are referred to as Dansgaard-Oeschger (D/O) events (Johnsen et al. 1992~~Dansgaard et al., 1993~~) and consist of rapid oscillations between cold Greenland stadials (GS) and warm interstadials (GI)~~- conditions~~. During some of the most extreme ~~Greenland stadials~~GS, North Atlantic marine sediment cores were found to contain layers of ice-rafted detritus (IRD) rich in detrital carbonate derived from Paleozoic bedrock that underlies~~ying~~ Hudson Strait (Heinrich, 1988; Broecker et al., 1992; Hemming, 2004). These so-called "Heinrich events" (Heinrich, 1988; Broecker et al., 1992) were attributed to massive discharges of icebergs from the Laurentide Ice Sheet to the North Atlantic via Hudson Strait, and in some cases, to a European origin (e.g. Grousset et al. 2000). ~~Greenland stadials (~~GS~~)~~ that contain Heinrich events are referred to as Heinrich stadials (HS). Freshwater forcing associated with Heinrich events weakened the Atlantic Meridional Overturning Circulation (AMOC) and the Intertropical Convergence Zone (ITCZ) moved south, resulting in periods of abrupt, substantial rainfall changes in the tropics and sub-tropics, referred to as "Tropical Hydroclimate Events"~~tropical hydroclimate events in the low latitudes~~ (Bradley and Diaz, 2021). Paleoclimate records from the northern Neotropics revealed that during those events, cool and dry conditions prevailed. For instance, such conditions were recorded in a speleothem record from Cuba, by a reduction in growth rates and a higher $\delta^{18}O$ values (Warken et al., 2019).

Lake Petén Itzá, northern Guatemala (Fig. 1), is located in a geologically and biologically diverse region that is climatically ~~highly biodiverse and geographically~~ sensitive ~~climate area~~ (Macario-González et al., 2022), ~~that is~~ affected by the annual migration of the ITCZ, trade wind intensity and moisture transport from the Caribbean Sea. The lake sediments represent one of the longest (~400 kyr) paleoclimate archives in the Neotropics (Kutterolf et al., 2016). ~~The sediments of this lake contain one of the oldest records in the region (75 kyr).~~ Few paleoclimate records from ~~Only a few nearby records in~~ the northern Neotropics are older than ~~exceed~~ 100 kyr ~~thousand years~~ in age (e.g. Lake Chalco, Central Mexico; Martínez-Abarca et al., 2021a). In addition, the relatively high sedimentation rate in Lake Petén Itzá enables high-temporal resolution sampling, making it possible to investigate abrupt, short duration climate changes such as GS and GI events during MIS3-2. This has been possible only for a few paleoclimate records from the Caribbean and the Gulf of Mexico region (e.g. Warken et al. 2020). For example, the Mg/Ca record from a speleothem in Cuba (Santo Domingo cave) documented relatively humid conditions during GI and drier climate during GS (Warken et al. 2019). GS were identified ~~For these reasons, Lake Petén Itzá has a unique sediment record with which to study abrupt climate change for stadial-interstadial events during MIS3-2. In~~ in earlier studies ~~-~~of ~~the~~ Lake Petén Itzá~~'s~~ sediments and suggested ~~,~~ ~~-~~that mean annual air temperature (MAAT) was 19-20°C, 6°C lower than the modern annual atmospheric temperature in the lowland northern Neotropics (Correa-Metrio et al., 2012). The cooler conditions were accompanied by high fire frequency around the lake (Correa-Metrio et al., 2012). I~~the i~~dentification of dry conditions during ~~these events~~HS were~~as~~ initially based ~~mainly~~ on the presence of gypsum ~~and clay~~ layers ~~as described by~~ (Hodell et al., ~~(~~2008;~~) and~~ Mueller et al., ~~(~~2010). Subsequent work ~~has~~ suggested an even greater decline in MAAT in the region during HS between 6 and 10°C (Hodell et al., 2012; Grauel et al., 2016). Evidence from an ostracod transfer function suggested Lake Petén Itzá experienced a decline in mean water temperature by 3°C (Cohuo et al., 2018; Pérez et al., 2021). Stable oxygen isotope measures on ostracod shells revealed low lake levels during HS, associated with dry conditions (Escobar et al., 2012). During HS1 (19-15 cal ka BP), one of the most studied periods in the Petén Itzá record, the presence of nektobenthic ostracod species such as *Cypridopsis okeechobei* and *Physocypria*

Con formato: Color de fuente: Automático

globula as well as the appearance of *Limnocythere opesta*, suggest a relatively cold lake with high primary productivity and lower water levels (Pérez et al., 2013). ~~been conducted including stable isotope geochemistry (Escobar et al., 2012; Hodell et al., 2012; Grauel et al., 2016; Mays et al., 2017), as well as biological indicators of climate change such as ostracods (Cohuo et al., 2018, 2020; Pérez et al., 2021), pollen and charcoal (Correa-Metrio et al., 2012). During HS, a drop in mean annual air temperature between 6 and 10°C compared with modern values has been reconstructed in the region (Hodell et al., 2012). Additionally, Lake Petén Itzá may have a reduction of up to 3°C in the mean water temperature according with recent ostracods based transfer function (Cohuo et al. 2018; Pérez et al., 2021). High salinities associated with a shallow lacustrine environment have been reconstructed based on ostracods data suggesting drier conditions. Moreover, stable isotope geochemistry reveals low lake levels during HS that caused Site PI-6 (water depth 71 m) to be within the epilimnion where oxygen concentrations are high (Escobar et al., 2012).~~ These cold and dry ~~environments~~ conditions promoted the establishment of savanna vegetation ~~such as~~dominated by ~~-~~Poaceae and Acacia, and in the lake, ~~, as well as~~ littoral cold-living ostracod~~s~~ species as *Cytheridella ilosvayi* and *Paracythereis opesta* were abundant (Pérez et al., 2021) ~~dominated the assemblage~~. ~~During GS, annual air temperature was between 19 and 20°C (Correa-Metrio et al., 2012) i.e. 6°C less than the modern annual atmospheric temperature in the region, accompanied by a high fire-activity around the lake.~~

~~This body of work at Lake Petén Itzá indicates that millennial change in climate and vegetation of Petén Itzá varied in concert with conditions in the North Atlantic expressed, such that colder, drier stadials (especially Heinrich stadials) and warmer, wetter interstadials occurred in Petén Itzá.~~

~~Despite the abundant e~~Previous paleoclimate and paleoenvironmental ~~and paleo-climate~~ information ~~regarding~~ about MIS3-2 was obtained primarily from Site PI-6 (water depth 71 m), one of the seven sites drilled in Lake Petén Itzá. Site PI-2, located 3 km east of Site PI-6 where the water depth is 54 m, showed a higher mean long-term sedimentation rates (~150 cm ka^{-1} vs. ~117 cm ka^{-1} at Site PI-2 and PI-6, respectively; Kutterolf et al., 2016). Therefore, millennial paleoclimate information was recorded at greater temporal resolution at Site PI-2, though the record covers a shorter time span (~56 kyr). Another advantage of Site PI-2 is that it lies in a flatter area and is thus less affected by episodic slumping that influence sedimentation rate. For this study, we used high-resolution geochemical and mineralogical data of sediments from Site PI-2 to explore hydrological variability in the northern Neotropics during MIS3-2 (59-15 cal ka BP). We compared our results from Lake Petén Itzá with other regional records to better understand potential impacts and drivers of climate shifts, particularly mechanisms that caused shifts in moisture transport to the northern Neotropics.~~gleaned from Lake Petén Itzá sediment records, responses of the lake to changes in runoff and evaporation, and related shifts in redox conditions have been analyzed mainly in only one of the seven cores drilled in Petén Itzá (Site PI-6; 71 water depth). Here we investigated Site PI-2, located 4 km to the east of Site PI-6 and in a water depth of 54 m, to test if the hydroclimate signals inferred from Site PI-6 were pervasively recorded in sediments throughout the lake.~~

~~The aim of this study is to investigate the hydrological response of Lake Petén Itzá to climate and environmental changes at Site PI-2 in the eastern lake basin (Fig. 1). We established an updated chronology for the sediment record from Site PI-2 in Lake Petén Itzá using existing AMS ^{14}C dates and non-linear age modeling. Moreover, we used high-resolution geochemical and mineralogical data to reconstruct hydrological changes for MIS 2 and 3 (59 to 15 cal ka~~

Con formato: Color de fuente: Automático

Con formato: Color de fuente: Automático

Con formato: Color de fuente: Automático

~~BP) including millennial climate oscillations such as HS, GI and GS. Results are compared with previous studies of Site PI-6.~~

2 Study area

2.1 Location and climate

Con formato: Color de fuente: Automático

Lake Petén Itzá is located in the northern lowlands of Guatemala (16°59'39.90"N, 89°49'21.07"W, 110 m above sea level [m asl]; Fig. 1). It has a surface area of ~100 km^2 and a maximum depth of 165 m (Hodell et al., 2006). The region has a humid tropical climate ("Af" according to the Köppen classification), with mean monthly air temperatures ranging from 22 to 30°C (INSIVUMEH, 2021). Mean annual precipitation is ~1600 mm (INSIVUMEH, 2021), but varies intra-annually, with a pronounced dry season from January to May, and a wet season that extends from late May through December. The climate of the northern Neotropics, particularly in terms of precipitation, is influenced by different climate forcing mechanisms that are still debated. First, the rain season is during the summer when the ITCZ is in its northernmost position. Second, the Caribbean Low-Level Jet (CLLJ), a region of maximum horizontal wind speeds (up to 16 m/s) at 925 millibars level, is linked to a precipitation maximum along the Caribbean and Central American coasts mainly between June and July (Amador et al., 2000). The CLLJ is a complex system responding to large-scale atmospheric changes, the Atlantic Warm Pool, as well as topographic effects and land-sea contrast in addition to variations in the sea surface temperature (SST) gradient between the eastern equatorial Pacific and Caribbean Sea (Spence et al., 2004; Wang, 2007). When the Pacific has higher temperatures than the Atlantic, the CLLJ intensifies towards the northern Caribbean, and consequently, precipitation increases at Petén (Whyte et al., 2008). Humidity can also be transported by the North American Monson (NAM) towards the north of Mexico from the Gulf of Mexico and the Caribbean, mainly during July, when atmospheric temperatures reach their maximum (Hu and Dominguez, 2015).

Con formato: Color de fuente: Automático

~~Maximum rainfall typically occurs in September, associated with tropical storms and hurricanes. The annual rainfall cycle is driven by the annual cycle of the latitudinal migration of the ITCZ, with dry conditions during winter when it is in the most southerly position, and wet conditions during summer when it is farther north. The region is also strongly influenced bythe NE Trade Winds that transport heat and moisture westward from the Atlantic toward the Caribbean Sea (Mestas-Nunez et al., 2005; Hodell et al., 2008).~~

2.2 Geology

~~The lake~~Lake Petén Itzá lies in a basin formed by asymmetric faulting (Fig. 1). To the north, marine carbonates of Paleocene-Eocene age outcrop, whereas to the south ~~the~~ surface rock~~s~~ ~~is~~ are composed of Cretaceous limestones (IGN, 1970). To the southeast, rocks ~~as well as~~and Quaternary alluvial sediments and soils ~~of alluvial origin~~ dominate, the latter ~~two~~ consisting mainly of carbonates and clays (Simmons et al., 1959; IGN, 1970; Mueller, 2009). The karst geology of the region~~area~~ promotes rapid infiltration of rainfall into the groundwater (Hodell et al., 2008), although a~~n~~ slow-flowing ephemeral stream at the southeast end of ~~the lake~~Lake Petén Itzá transports water and sediment into the lake basin ~~waterbody~~ during the rainy season.

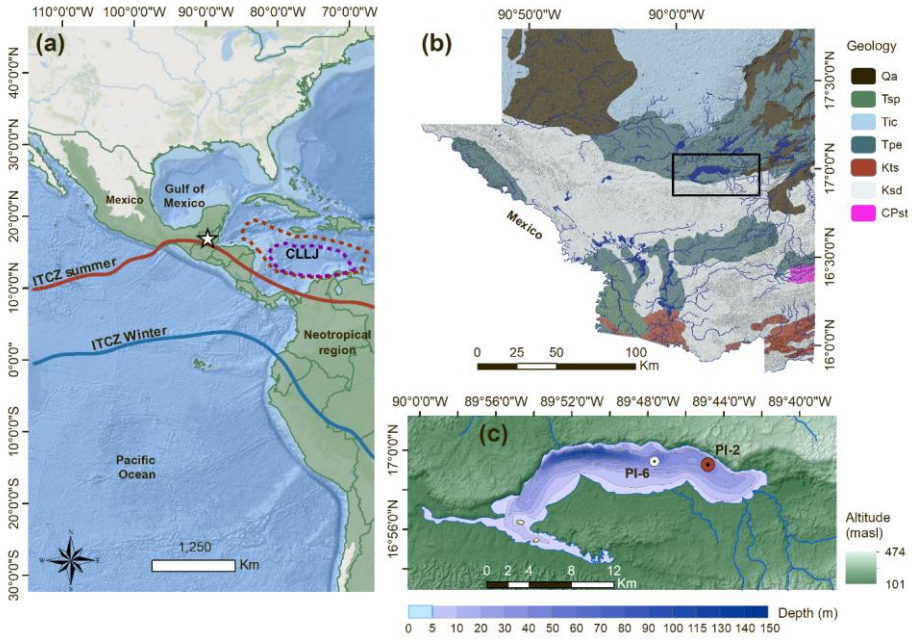

Figure 1. ~~Geographic map with the l~~Location of Lake Petén Itzá, along with regional climatological and geological information. ~~A~~a) Location of Guatemala in Central America and geographic position of the lake (white star). ~~The~~ Neotropical region (green), ITCZ positions during summer (red) and winter (blue). The extent of the CLLJ is summer (red) and winter (blue) is shown. The dotted lines represent the zonal easterly winds larger than 16 m/s at 925 millibars level associated with the CLLJ. ~~is shown in green. ITCZ positions during summer and winter are shown. The warm Caribbean surface current is indicated.~~ Service Layer Credits: Esri, Garmin, GEBCO, NOAA and NGDC ~~, and other contributors~~ (2022). b~~B~~) Overview of ~~G~~geology in northern Guatemala and location of ~~and hydrology of the~~ Lake Petén Itzá (black rectangle) region: ~~. The black rectangle indicates the position of Lake Petén Itzá.~~ Qa) Quaternary alluvium, Tsp) Tertiary upper Oligocene-Pliocene, Tic) Eocene sedimentary rocks, Tpe) Paleocene-Eocene marine sediments, Kts) Cretaceous-Tertiary clastic sediments, Ksd) Cretaceous carbonaceous rocks, CPst) Carboniferous-Permian sand conglomerate (geological information: IGN, 1970). ~~C~~c) Digital elevation model, principal rivers and streams, and ~~around the lake, principal fluvial streams and~~ bathymetry of Lake Petén Itzá, location of core sites: ~~the~~ PI-2 (red dot) and PI-6 (white dot). ~~location is indicated by the red dot while PI-6 by the white point.~~

~~2~~3 Methods

~~2.1~~3.1 ICDP drilling campaign

During February and March 2006, multiple cores were drilled at seven locations in Lake Petén Itzá (PI-1, PI-2, PI-3, PI-4, PI-6, PI-7 and PI-9) as part of ~~an~~ International Continental Scientific Drilling Program (ICDP) project [PISDP]. ~~The m~~Maximum drilling depth, ~~reached~~ 133 m, was achieved at Site PI-7. Sediment~~ology lithology~~, magnetic susceptibility and density data for the cores were presented by Hodell et al.~~,~~ (2006, 2008) and Mueller et al.~~,~~ (2010).

Here, we focus on the sediment sequence recovered from ~~Site~~ Site PI-2. The site displayed a relatively high mean sedimentation rate (~150 cm ka^{-1}; Kutterolf et al., 2016) and an average ~~sediment~~ core recovery of 86.3%, which enabled climate and environmental studies at ~~permitted the reconstruction of climate change at~~ high temporal resolution. The PI-2 sequence was retrieved from a water depth of 54 m in the eastern part of the lake (16°59'58.04"N, 89°44'41.51"W, Fig. 1c~~C~~). The drill site receives~~s~~ detrital material in the form of colluvium from ~~that comes off~~ the steep northern shore. Five holes were drilled at S~~S~~ite PI-2, the longest of which reached a ~~maximum~~ sediment depth of ~~82~~ 67 m. The composite sequence at ~~Site~~ Site PI-2 was divided into 11 lithostratigraphic units based on changes in facies composition (Mueller et al., 2010). For this study, we analyzed sediment samples from Units 6 to 2 (67-19 m depth), which span the interval of MIS3-2 (Correa-Metrio et al., 2012; Escobar et al., 2012).

Table 1. AMS ^{14}C dates and ages of tephra used for the age-depth model. Data with an asterisk (*) are measurements of terrestrial organic matter (i.e. woody debris, Mueller et al., 2010) ~~reported by Mueller et al., (2010)~~. Data with double asterisk (**) are tephra~~s~~ layers ~~reported by (~~Kutterolf et al., ~~(~~2016). All radiocarbon dates were calibrated using a Bayesian model (Blaauw and Christen, 2011) and the IntCal20 curve (Reimer et al., 2020). "avg" refers to the mean age obtained from two dates in the same sample.

labID	~~Site~~ Core, section cm	Depth (m)	Age (^{14}C ~~a~~yr)	± (1σ)	Mean (cal yr BP)	Modelled age range (cal yr BP)
144277*	2D-1H-1, 14	0.22	425	30	22	-60 – 150
139341*	2D-2H-2, 25	4.88	1715	35	1620	1516 – 1737
139342_avg*	2B-4H-2, 39	10.25	3740	33	4043	3655 – 4169
144270*	2A-5H-1, 87	10.85	4280	30	5203	4903 – 5288
139344_avg*	2B-5H-1, 102	12.45	7468	40	8276	8170 – 8390
139346*	2D-5H-1, 56	12.76	7835	30	8736	8614 – 8875
139399*	2B-6H-2, 41	16.43	11135	40	13057	12909 – 13168
139399*	2D-6H-2, 44	17.46	11880	35	13637	13439 – 13792
144272*	2A-8H-1,96	20.44	13095	40	15710	15497 – 15907
139400*	2D-8H-1, 5	21.65	13480	45	16197	16059 – 16326
139401_avg*	2B-8H-1, 132	22.24	13533	45	16408	16225 – 16600
139402*	2B-9H-1, 146	25.47	15355	50	18632	18321 – 18820
144274*	2B-10H-2, 98	29.59	19740	70	23904	23535 – 24236
144269*	2A-12H-1, 47	31.49	21940	80	26176	25932 – 26661
139403*	2B-12H-1, 121	38.41	25540	160	35488	32614 – 37722
139404*	2A-14H-1, 115	40.38	32680	980	36947	34181 – 38962
139405*	2A-16H-1, 66	44.55	34380	450	39794	38469 – 40926
139406*	2C-2H-1, 135	47.08	38760	740	42621	41955 – 43422
139407*	2A-17H-1, 104	48.06	41350	1020	43944	42974 – 44960
139343*	2A-17H-1, 151	48.4	41600	900	44195	43186 – 45263
C1**	2B-5H-2, 65	13.09	9805	100	9378	9231 – 9550
C2**	2A-7H-1, 131	17.69	13158	100	13761	13537 – 13959
C4**	2A-19H-2, 10	54.46	49100	2000	48793	45957 – 52137
C5**	2C-9E-1, 114	64.22	53000	3000	55826	51080 – 62132

3.2 Age-depth model

Previous studies used slightly ~~established~~ different chronologies for the sediment sequences from Lake Petén Itzá ~~sediment sequences~~, with a focus on the composite section from S~~S~~ite PI-6. ~~These~~ Those studies used linear interpolation between radiocarbon dates (Hodell et al., 2008; Mueller et al., 2010), projection onto the PI-6 sequence of AMS ^{14}C dates from other cores (Escobar et al., 2012), and ~~dates~~ ages of tephra layers (Kutterolf et al., 2016). Mays et al., (2017) constructed a Bayesian age model for Site PI-6. We similarly refined the age-depth model for PI-2 using a Bayesian model (Blaauw and Christen, 2011). In this model (PETEN 02), we used 20 radiocarbon ages reported by Mueller et al.~~,~~ (2010) and Escobar et al.~~,~~ (2012), together with four dated tephra layers~~s~~ ~~preserved~~ in the PI-2 sequence (Kutterolf et al., 2016; Table 1). Radiocarbon ages were calibrated using the IntCal20 curve (Reimer et al., 2020). The model was established using the Bacon package (Blaauw and Christen, 2011) ~~in~~ of the R-Studio software (v. 4.2). An initial sedimentation rate of 1 mm yr^{-1} (100 cm ka^{-1}) and 28 segments along the core were assumed. Processes that deposit material rapidly at the bottom of the lake, such as turbidite flows and volcanic ashfalls, can confound the chronology by contributing substantial amounts of material in a short time span (Moernaut et al., 2017; Mulder et al., 2019). Hence, we excluded 31 such deposits during ~~the~~ age modeling, including carbonaceous turbidites and tephra layers~~s~~, identified using the descriptions of Mueller et al.~~,~~ (2010~~;~~) ~~(~~ Appendix A).

3.3 X-Ray fluorescence sediment analysis ~~(XRF)~~

X-Ray fluorescence (XRF) measurements were carried out at the University of Minnesota, Duluth, using a Cox Analytical Itrax Core Scanner (Cr-Tube, 30 kV, 55 mA, 15 s exposure) with a resolution of 1 cm. Particular focus was given to titanium (Ti), aluminum (Al), calcium (Ca), iron (Fe) and manganese (Mn) because these elements~~they~~ are ~~suitable~~ reliable indicators of runoff (Ti, Al), evaporation (Ca) and redox conditions (Fe, Mn). Data from XRF, in ~~as~~ counts per second (cps), ~~–~~were processed using a centered log-ratio transformation, ~~calibrated using a log-ratio calibration~~ following ~~Weltje and Tjallingii (2008) and~~ Weltje et al.~~,~~ (2015). Centered log-ratio-transformed (CLR) compositional data express elemental quantities in terms of actual concentrations ~~Log-ratio calibration~~and incorporate~~s~~ uncertainties acquired during core scanning such as ~~the~~ sediment water content ~~in the sediment~~, grain size, and irregularities ~~in~~ of the sediment surface (Dunlea et al., 2020). For each XRF measurement, we divided an element (e.g. $Ti_{(cps)}$) by ~~a~~ the geometric average of the geochemical set (Ti, Al, Ca, Fe and Mn)~~common denominator that was measured simultaneously in the XRF spectra (e.g. $Ti_{(cps)}/Inc_{(cps)}+Coh_{(cps)}$). We selected the sum of the Incoherent and Coherent scattering as the common denominator because they reflect changes in the water content and density of the sediments (Kylander et al., 2011; Marshall et al., 2011)~~. The natural logarithm of the ratio was then calculated [e.g. ln ($Ti_{(cps)}$/ Geometric Average~~Inc+Coh$_{(cps)}$~~)]. Calibration was carried out using Xelerate software (Bloemsma, 2015; Weltje et al., 2015). A principal component analysis was carried out with CLR data (PCA; Appendix B) to distinguish the processes that control each element. The PCA results are given in Appendix B. We used these results to define the Ca/(Ti+Fe) ratio as an indicator of evaporation and the Mn/Fe as a proxy of redox processes (Wersin et al., 1991; Yarincik et al., 2000). Simultaneously, a ~~Data as cps and log-ratio calibrated can be found in the Appendix B. A~~ LOESS smoothing function was applied to the CLR data to dampen the noise signal from measurement errors or anomalous data. LOESS smoothing was carried out in R-Studio (v. 4.2) (R Core Team, 2018) with a span value of 3.

Con formato: Color de fuente: Automático

Con formato: Color de fuente: Automático

3.4 X-Ray Diffraction for sediment mineral analysis ~~(XRD)~~

To document changes in sediment mineralogy, 100 samples from Site PI-2 cores were used for X-ray diffraction (XRD) analysis. Sampling was carried out at irregular intervals ranging from 0.5 to 1.0 m. Sediment samples were dried at room temperature and ground with a mortar and pestle. Measurements were conducted with a Rigaku Miniflex 600 (15mA/40kV) XRD at the Department of Physical Geography, Freie Universität Berlin. Peaks obtained from 3 to 80° of rotation were identified with X-Pert High Score (Version 1.0b) from Philips Analytical. The peaks were calibrated against the main quartz peak (I100) at d=3.34 Å. Diffraction potential files of the International Center for Diffractometric Data, USA, were used as reference for the identification of the different mineral phases. The quartz and gypsum counts, the sum of montmorillonite+vermiculite (clay) and the sum of calcite+dolomite+aragonite+magnesium calcite (carbonate) were ~~summed~~ added and the relative percentages were calculated as follows: Mineral [%] = (Mineral count*100)/Σ Minerals (Last, 2001).

3.4 Geochemistry of ~~B~~bulk ~~geochemical measurements~~ sediment

Analyses of total carbon (TC), total organic carbon (TOC), total inorganic carbon (TIC) and total nitrogen (TN) were carried out on the same sediment samples used for XRD. All measurements were performed at the Department of Geological Sciences, University of Florida, Gainesville. TC and TN were determined with a Carlo Erba NA1500 CNHS Elemental Analyzer. TIC was measured coulometrically (Engleman et al., 1985) with a UIC CO_2 coulometer 5011 (Coulometrics) coupled with an AutoMate preparation device. TOC was calculated as the difference between TC and TIC. TOC/TN ratios are reported on a molar basis.

~~3~~4 Results

~~3.1~~4.1 Chronology

Data presented in this study cover the depth interval from 67 to 19 m of the PI-2 record, corresponding to an age range from 59 to 15 cal ka BP (Fig. 2). From the sediment surface to 51 m depth, average age uncertainty is ±0.8 ka. The uncertainty of the chronology increases in the deeper~~st~~ sediment intervals, especially below 51 m depth (>46 cal ka BP), ~~reaching~~ resulting in ±6.7 ka at the bottom of the sequence (67 m sediment depth). There were two intervals during which ~~instantaneous~~ event deposits (mainly carbonaceous turbidites) were abundant: between 67 and 48 m sediment depth (58.5-43.8 cal ka BP) and from 23 m to 19 m (16.6-15 cal ka BP) continuing to the sediment surface ~~0 m depth (16.6-0 cal ka BP)~~. Our age-depth model differs from the one ~~in~~ by Kutterolf et al.~~,~~ (2016) mainly in the interval between 40 and 34 cal ka BP, where ages calculated by our model are as much as 2 ka younger. ~~However, t~~This is, however, within the average uncertainty of our age model at these depths (greater than ±2.3 ka).

~~3.2~~4.2 Climate proxies

Results are presented by age and according to the lithostratigraphic units proposed by Mueller et al.~~,~~ (2010; Fig. 3; ~~Table 2~~Appendix B). CLR values for Ti ~~log ratio values~~ vary between ~~-5~~2.~~1~~6 (low runoff) and +1.6~~ 1.2~~ (high runoff) throughout the sequence, with an average of -0.1±0.3 ~~-2.2±0.7~~ (Fig. 3). In Units 6 and 5, Ti is characterized by fluctuating values ~~compared to the rest of the sequence, in which values~~ ranginge between -1.6 and +0.7~~ 5.6 and -1.2~~.

Lowest average values (≤ -2.81) were observed in Unit 4. Units 3 and 2 display the highest Ti content, both with maxima of +1.1 ~~1.3~~.

$CaCO_3$ ~~data~~ values obtained by XRD vary from 4.2 to 75.0%, with an average of 33.9±15.3%. Units 6 and 5 show similar values of $CaCO_3$, oscillating between 8.7% and 73.4% (mean 40.7±12.4%). A reduction in the $CaCO_3$ content characterizes Unit 4 ~~reaching up~~with an average of 28.9±14.9%. In Unit 3, data vary from 26.3% ~~and~~ to 58.7% (mean = 34.7±7.5%). ~~During~~ Unit 2, with an average of 20.9±17.9%, is characterized by , a slight ~~average~~ decrease in $CaCO_3$ content ~~(mean = 20.9±17.9%) dominates,~~ but shows a maximum ~~finishing with a~~ of ~~peak up to~~ 75.0% at 15.5 cal ka BP.

CLR values of Ca/(Ti~~+Al~~+Fe) ~~log-ratios~~ range from -0.1 (low evaporation) to +6.~~3~~ 4 (high evaporation) throughout the sequence, with an average of ~~2.8~~+3.0±1.0 (Fig. 3). In Units 6 and 5, Ca/(Ti~~+Al~~+Fe) ~~ratios are~~is variable (±0.7 to +5.~~6~~9), with three pronounced peaks of ~~4.9~~+5.2 (51.9 cal ka BP; 58.9 m), +5.~~6~~8 (46.1 cal ka BP; 50.8 m) and +5~~4.8~~4 (40.3 cal ka BP; 45.3 m). The ratio increases in Unit 4 and ranges from +1.54 to +5.9~~6.3~~ (mean = +3.64±0.7). Unit 3 displays the lowest Ca/(Ti~~+Al~~+Fe) ~~ratios~~, varying between -0.1~~6~~ and ~~3.3~~+4.0 (mean = +1.~~7~~9±0.45). Unit 2 is characterized by highly variable Ca/(Ti~~+Al~~+Fe) ~~ratios~~, ranging between -0.1 and +6.~~0~~4 (mean = +3.~~2~~3±1.4), and shows highest ~~ratios~~ values of up to ~~<~~+6.~~0~~4 at the top of the ~~sequence~~investigated interval.

The mineralogical composition of the Lake Petén Itzá record obtained by XRD is dominated by carbonates, including calcite, dolomite, aragonite and magnesium calcite. About 65% of the sediment samples contained more than 50% carbonate, with calcite (mean 45.9±2.7%) and dolomite (mean 13.4±1.3%) being most common. Quartz shows highest average values in Units 6 (3.0±1.5%), 5 (3.2±2.0%) and 3 (5.1±2.5%). The clay content (montmorillonite+vermiculite) is highly variable throughout the record, ranging from 0 to 13.7% (mean 3.6±3.0%). It shows a gradual decrease from Unit 6 (4.5%) to Unit 4 (2.1%). Unit 3 contains the highest clay content (mean 8.5±2.9%), but decreases upward to an average of 1.9% in Unit 2. The gypsum content is highly variable and ranges from 0 to 100%, with an average of 32.6±3.6% (Fig. 3). Units 6, 5 and 3 show the lowest gypsum content of the record, with average values of 5.1%, 14.9% and 6.2%, respectively. In Unit 5, maxima of 96.8 and 77.7% occur at 50.9 cal ka BP (56.8 m) and 46.3 cal ka BP (51.1 m), respectively. In Units 4 and 2, ~~there is~~ a ~~strong~~ large increase in ~~the~~ gypsum content is observed, with average values of 53.9 and 78.2%, respectively.

TOC values vary between 0.2 and 6.1%, with an average of 2.1±1.1% throughout the sequence (Fig. 3). In Unit 6, TOC values range from 1.1 to 4.5% ~~in Unit 6~~. Unit 5 displays TOC values that range from 0.5 to 6.1%, and ~~significantly~~ decrease substantially around 47.2 cal ka BP (52.3 m). From 37.8 to 30.9 cal ka BP (42.0 to 35.0 m depth) in Unit 4, three distinct maxima with TOC values of 3.7% (37.3 cal ka BP; 41.1 m), 5.2% (35.4 cal ka BP; 38.4 m) and 3.4% (33.0 cal ka BP; 36.5 m) were determined. The TOC content in Unit 3 increases to a maximum of 3.7%, with an average of 2.2±0.6%. Unit 2 is characterized by lower TOC values, which vary from 0.2 to 2.5% (mean 0.7±0.4%).

Molar TOC/TN ratios range from 4 (high aquatic organic matter content) to 38 (high terrestrial organic matter content) throughout the record (mean 16.8±6.3). Unit 6 shows TOC/TN ratios that average 10.7±3.2, with a gradual increase to 18.9 at the top of the unit (Fig. 3). Units 5 and 4 display similar TOC/TN ratios, ranging between 4.4 and 38. Four maxima of 31.3 (51.8 cal ka BP; 58.6 m), 35.9 (46.4 cal ka BP; 51.0 m), 27.4 (40.4 cal ka BP; 45.3 m) and 38 (31.9

Con formato: Subíndice

Con formato: Subíndice

cal ka BP; 35.7 m) were identified, as were minima of ~6.8 between 40.3 and 39.2 cal ka BP (45.2-43.9 m depth). At the top of Unit 4 (31.0-23.4 cal ka BP; 35.0-29.0 m depth), TOC/TN ratios decrease gradually from 26.1 to 10.8. Units 3 and 2 have the lowest values of the entire sequence, ranging between 4.6 and 17.5, with a slight increase to 20.9 at the top of Unit 2.

CLR values of Mn/Fe ratios ~~log ratios~~ range between ~~-5.5~~ -7.4 (~~rather~~ anoxic) and +0.2 ~~-1.3~~ (~~rather~~ oxic), with an average of -3.4±0.5~~6~~ throughout the record (Fig. 3). Unit 6 displays the lowest values of the sequence varying between -6.6~~4.2~~ and -2.7. Unit 5 presents a gradual increase in ~~the~~ Mn/Fe ratios~~ratios~~ between 52.7 and 46.1 cal ka BP (60.0-50.8 m), reaching as high as ~~up to~~ -1.3~~1~~. Units 5 and 4 show similar values, which vary from ~~-5.5~~7.4 to + ~~-1.3~~0.2, with maxima of ~~-1.3~~+0.2 (46.2~~1~~ cal ka BP; 50.8 m), -1.6~~2.1~~ (40.3~~2~~ cal ka BP; 45.3 m), -1.7~~9~~ (37.1 cal ka BP; 40.5 m) and -~~1~~0.7~~8~~ (29.6 cal ka BP; 34.3 m). In Units 3 and 2 values fluctuate between -7~~4~~.5~~3~~ and -2~~3~~.6~~1~~ (-3.7~~8~~±0.5~~3~~).

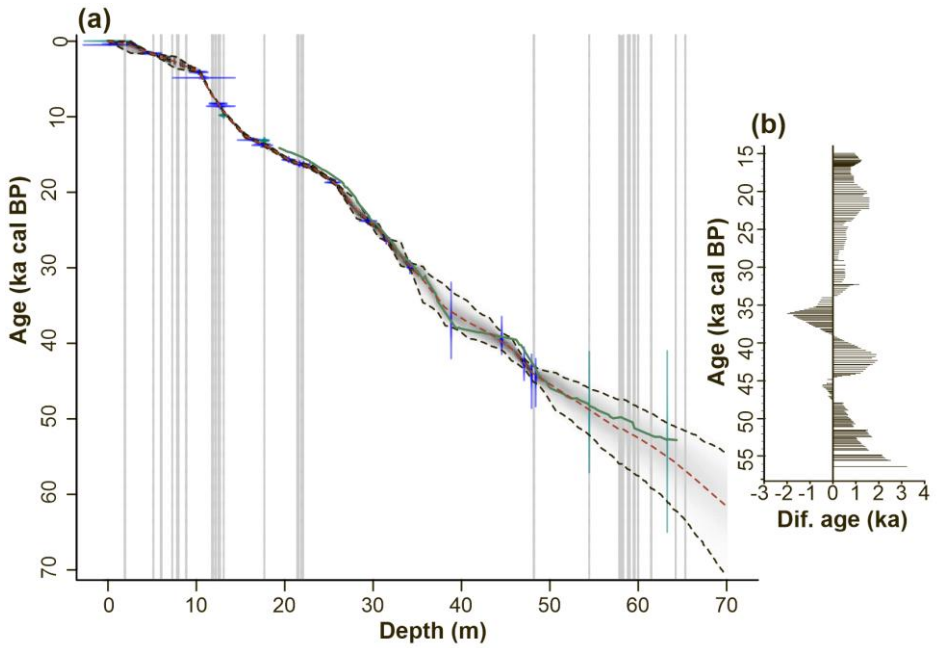

Figure 2. Age-depth model ~~obtained~~ for the PI-2 record: ~~A~~a) ~~Model parameters estimated by (from left to right) the quantity of iterations in each section, range of accumulation rate and memory (how much the accumulation rate of a particular depth in the core depends on the depth above it; 1=100% memory); B)~~ Chronology of the PI-2 record. Gray vertical lines indicate the location of the 32 instantaneous deposits that were removed for the modelling. Ages and their uncertainties are indicated in blue. ~~Red~~Green-solid line shows the chronology obtained by Kutterolf et al.~~,~~ (2016) and used ~~in~~ by Cohuo et al.~~,~~ (2018, 2020). The ~~R~~red-d~~ashed~~~~otted~~ line represents the average age, ~~while~~ whereas the black-~~dotted~~ dashed line~~s~~ ~~is~~ are the minimum and maximum range ~~of~~ for each age. ~~C~~b) Age difference between the model~~s~~ ~~of~~ used in this study and the one presented by Kutterolf et al.~~,~~ (2016) in the interval

Con formato: Color de fuente: Automático

betweenbetween 59 and 15 cal ka BP. The dData were calculated as follows: Dif. Aage (ka)s = aAges this study - ages reported by Kutterolf et al., (2016).

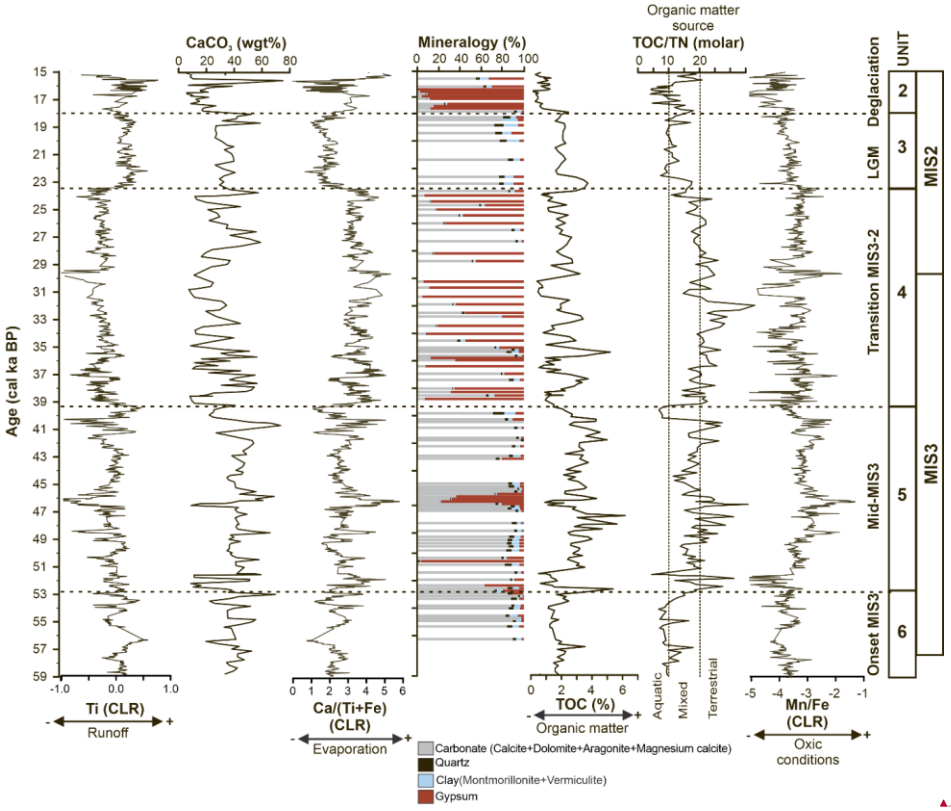

Figure 3. Comparison ofSediment variables in proxy records of the PI-2 sequence betweensequence, between 59 andto 15 cal ka BP. Black horizontal dotted lines indicateing periods that coincide with unit boundaries described by Mueller et al., (2010). The timing for of the transitions of MIS3-2 transition and the Last Glacial Maximum (LGM) isare shown on the right (Lisiecki and Raymo, 2005). Runoff and evaporation are indicated by Ti centered log-ratio (CLR) values and Ca/(Ti+Al+Fe) ratios log-ratios, respectively. CaCO3 Carbonate ($CaCO_3$) content is shown as percentage dry weight (%wgt). Percentage of quartz, clay (montmorillonite+vermiculite) and gypsum are shown. Total organic carbon is anas indicator of primary productivity, Total total organic carbon to total nitrogen (TOC/TN) ratios asare indicators of organic matter sources, and the CLR value of Mn/Fe ratiosis used as as proxy for redox conditions.

Con formato: Color de fuente: Automático

Con formato: Color de fuente: Automático

Con formato: Color de fuente: Automático

Con formato: Color de fuente: Automático, Subíndice

Con formato: Color de fuente: Automático

45 Discussion

The discussion of the Lake Petén Itzá paleoenvironment focuses on three key objectives: 1) hydrological variability during MIS3-2 and millennial oscillations (GS, GI and HS) recorded at Site PI-2, 2) comparison of our Site PI-2 data with previously reported data from Site PI-6, and 3) identification of potential climate forcing mechanisms that may have provided humidity to the Petén area through transregional proxy comparison. Our mineralogical and geochemical data are presented and interpreted according to the five periods that correspond to lithological Units 6-2 proposed by Mueller et al. (2010) (Appendix C): a) onset of MIS3, b) mid-MIS3, c) transition MIS3-2, d) last glacial maximum, and e) deglaciation. The lithological units were based on sedimentology and stratigraphy and verified with core-logging data (density, magnetic susceptibility) and with seismic reflection profiles throughout the Lake Petén basin. ~~Our mineralogical and geochemical analyses enabled us to define five units (Units 6-2) that correspond to the lithological classification of Mueller et al., (2010) (Table 2). Each unit corresponds to different stages in the lake evolution during MIS3 and MIS2 (59-15 cal ka BP). In the following section, we discuss the environmental and hydrological conditions that prevailed in and around Lake Petén Itzá during the deposition of each unit.~~

~~***Table 2.*** *Main lithological characteristics of Units 6 to 2 discussed in this study and previously defined by Mueller et al., (2010). We present the depth interval covering each unit, as well as the age interval calculated in this study.~~

5.1 Hydrological and environmental ~~conditions~~ responses during MIS3-2

5.1.1 Onset of MIS3 ~~Unit 6~~ (59-52.7 cal ka BP): High runoff and low evaporation ~~in the lake at the onset of MIS3~~

~~Unit 6~~ The onset of MIS3 corresponds to ~~Unit 6.the onset of MIS3.~~ Ti is widely used as indicator for runoff (Mason and Moore 1982; ~~Yarincik et al., 2000;~~ Davies et al., 2015). High Ti ~~log-ratio values~~ (up to 0.7~~-1.1~~) in this unit suggests high runoff, particularly around 56 cal ka BP (Fig. 3). This is supported by concomitantly high clay and quartz content, with averages of 4.5 and 3.0%, respectively. Clay minerals, particularly ~~such as~~ montmorillonite and vermiculite, are generated during chemical weathering of unstable siliciclastic minerals such as plagioclase, especially in tropical regions where atmospheric humidity is high, resulting in the enrichment of quartz (Weltje, 1994; Boggs, 2006; Van De Kamp, 2010). ~~Lake Petén Itzá is located in a karst region (IGN, 1970).~~ Quaternary alluvial sediments ~~in the southeast~~ could be the source of siliciclastic minerals (Simmons et al., 1959; Mueller, 2009). ~~W~~We suggest that the high clay and quartz content in Unit 6 is indicative of wet~~ter~~ conditions, which provided abundant runoff to the lake. ~~compared to the less humid environment reconstructed for the end of MIS3 (48-23 cal ka BP) in previous studies at Site PI-6 (Hodell et al., 2008). Furthermore, the clay abundance in Unit 6 could be enhanced by the increase in precipitation and high rates of chemical weathering.~~ Ca provides information on supersaturation and precipitation of ions in solution, triggered by high evaporation (Engstrom and Wright, 1984; Boyle et al., 2001). Ca in lake sediments, however, can also originate from detrital inputs in karst regions such as in Petén, and from biogenic sources, i.e., shell formation by mollusks and ostracods and CO_2 withdrawal by plants for photosynthesis. Therefore, we normalized Ca values to indicators of detrital input such as Ti and Fe (Appendix B), and used the Ca/(Ti+Fe) as an indicator for past variability of evaporation (Mason and Moore, 1982; Yarincik et al., 2000). Low Ca/(Ti+Fe) ratios (mean 2.3±0.6) and

Con formato: Color de fuente: Automático

Con formato: Color de fuente: Automático

gypsum content (mean 5.0±5.1%) at the onset of MIS3 indicate low evaporation of lake water and more humid conditions, with only a few intermittent dry periods, at ~55.1 and 53.8 cal ka BP (Fig. 3).

The TOC/TN ratio has long been used as~~s an~~ indicator for the source of organic matter in lacustrine sediment sequences (Talbot and Johannessen, 1992; Meyers and Ishiwatari, 1995). ~~During~~In the interval between 59-53 cal ka BP, low TOC/TN ratios (mean 10.7±3.2) indicate that the sedimentary organic matter ~~wa~~is predominantly of aquatic origin (Meyers et al., 2003). The Mn/Fe ratio is used to infer variations in redox conditions in lakes (Wersin et al., 1991; Naeher et al., 2013; Friedrich et al., 2014; Ortega-Guerrero et al., 2020). Lower values of the Mn/Fe ratio generally indicate low concentration of O_2 in the water column, which is explained by more rapid reduction of Mn compared to Fe under anoxic conditions favoring preferential Mn deposition. In contrast, higher values of the Mn/Fe ratio suggest high levels of O_2, as Fe oxidizes faster than Mn in oxic environments. Low Mn/Fe ratios (mean -3.7±0.3) indicate anoxic conditions in the lake's bottom waters. Anoxia may have been associated with a high-water level (as is observed today), which likely prevented wind-driven mixing of the water column.

High values of magnetic susceptibility measured at Site PI-6 (Fig. 4) support our interpretation of a wet climate compared to the less humid environment inferred for the end of MIS3 (48–23 cal ka BP; Hodell et al., 2008). Previously reported ostracod data from Sites PI-2 (Cohuo et al., 2020) and PI-6 (Pérez et al., 2021) are consistent with substantial precipitation in the study area during the deposition of Unit 6, and are associated with high water levels, reflected by the dominance of *Cypria petenensis*. Moreover, the low content of terrestrial organic matter at Site PI-2 is consistent with the pollen-based inference for extensive grasslands around Lake Petén Itzá, indicating relatively little terrestrial plant biomass in the watershed (Bush et al., 2009; Fig. 4). Absence of arboreal vegetation, contemporary with the highest deposition of aquatic organic matter in our record during the onset of MIS3, was likely associated with winter rains from north cold fronts that caused lake levels to increase (Hodell et al., 2008), leading to a more distal position of the coring site.

Con formato: Color de fuente: Automático

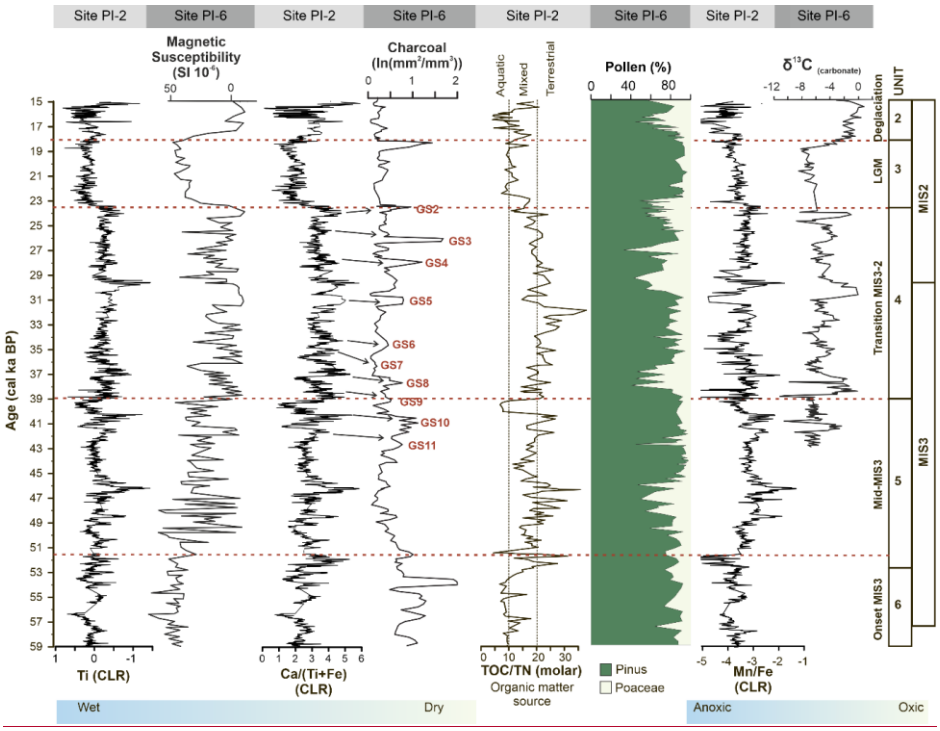

385 **Figure 4.** Sediment variables in cores from Sites PI-2 and PI-6 (3 km to the west [Fig. 1]) Centered log-ratio (CLR) values of Ti, Ca/(Ti+Fe) and Mn/Fe, TOC/TN and magnetic susceptibility (Hodell et al., 2008), Pinus/Poaceae pollen and charcoal datasets (Correa-Metrio et al., 2012) as well as $\delta^{13}C$ values from ostracod valves (Escobar et al., 2012). Brown dashed lines indicate unit boundaries described by Mueller et al. (2010).

~~This is consistent with ostracod data provided by the PI-2 record that indicate substantial precipitation in the study area~~
390 ~~during the deposition of Unit 6 (Cohuo et al., 2020).~~

~~Ca provides information on the supersaturation and precipitation of ions in solution, triggered by high evaporation (Engstrom and Wright, 1984; Boyle et al., 2001). Ca in lake sediments, however, can also originate from detrital inputs in karst regions such as the Petén as well as by authigenic formation at the lake bottom. Therefore, we normalized Ca values by indicators of detrital input such as Ti, Al and Fe, and used the Ca/Ti+Al+Fe log-ratio as an indicator of past~~
395 ~~variability in evaporation (Mason and Moore, 1982; Yarincik et al., 2000). Low Ca/Ti+Al+Fe log-ratios (mean 2.1±0.6) and gypsum content (mean 5.0±5.1%) in Unit 6 indicate low evaporation of lake water and more humid conditions, with only a few intermittent dry periods, at ~55.1 and 53.8 cal ka BP (Fig. 3).~~ Predominantly wet conditions during the onset of MIS3, like those inferred from Lake Petén Itzá sediments, ~~have~~ also been reported~~inferred~~ from other sites ~~for that time~~ in the northern Neotropics (Fig. 45) using geochemical records. They include ~~from~~ Lakes
400 Chalco, ~~(~~central Mexico~~;~~ (Martínez-Abarca et al., 2021b) and Babicora, ~~(~~northern Mexico ~~(;~~ Roy et al., 2013). In

Con formato: Color de fuente: Automático
Con formato: Color de fuente: Automático
Con formato: Color de fuente: Automático

contrast, pollen and sedimentological information from Lake Fúquene (Colombia) indicates moderately dry conditions and a reduction in lake ~~-~~surface area associated with a decline in precipitation in northern South America (Groot et al., 2013). Differences in precipitation between the northern and southern limits of the American tropics were likely associated with the latitudinal ~~(northward) migration~~position of the ITCZ (~~Fig. 5~~Jaeschke et al., 2007; Gibson and Peterson, 2014; Martínez-Abarca et al., 2021b; Lozano-García et al., 2022).

Reflectance data from ~~the~~ marine sediments collected in ~~of~~ the Cariaco Basin, off Venezuela (Deplazes et al., 2013), and $\delta^{18}O$ data from marine record MD02-2529 retrieved from ~~in~~ the Eastern Equatorial Pacific (Leduc et al., 2007) indicate a more northerly position of the ITCZ during this period. Hodell et al. (2008) suggested that increases in runoff in Petén Itzá co-occurred with increases in SST in the subtropical northeast Atlantic (Site SU8118, Portugal; Bard et al., 2000). SST between sites in the region, however, have not yet been considered. Therefore, we compared the Ti data from Site PI-2 with the SST difference (ΔSST) calculated between Site MD02-2529 in the eastern Pacific (Leduc et al., 2007) and ODP Site 999A in the Caribbean (Schmidt et al. 2006; Fig. 6). It should be noted, though that the ΔSST provides considerable uncertainties associated with the prediction error of the quantitative estimation of SST in both records, their age-depth models, as well as the calculation of Δ itself due to the use of different temperature proxies (Mg/Ca planktonic foraminifera for ODP-999A, and alkenone $U^{K'}_{37}$ for MD02-2529) and temporal resolutions. Even with these limitations, the ΔSST record used as a CLLJ proxy for variations in the strength of the CLLJ shows an apparent coupling of the ΔSST with the low-frequent variations recorded in our Ti data (Fig. 6). Decreases is ΔSST indicate that the Caribbean SST was lower than the one in the Pacific. This could have promoted an increase in the intensity of the CLLJ since a cold Caribbean favors the expansion of the North Atlantic Subtropical High displacing the CLLJ to the west and increasing the humidity in Petén Itzá (Wang, 2007; Lachniet et al. 2009; Fig. 7). During the early MIS3, ΔSST decreased and it got drier until ~45 cal ka BP. After that, the ΔSST increased and wetter conditions occurred around the lake. Although the strength of the CLLJ does not solely depend on the ΔSST between the eastern Pacific and the Caribbean, but also depends on the regional topography, the position of the ITCZ, as well as the expansion/contraction of the North Atlantic Subtropical High (NASH; Wang, 2007), we find clear evidence for a close relationship between ΔSST and Ti and hence runoff to Lake Petén Itzá regarding low-frequent variations. This implies, that in addition to changes in the ITCZ, spatiotemporal changes are linked to variations in CLLJ steering the influx of moisture into Petén during MIS3-2. Additionally, despite the fact that there is no evidence for the variability of the NAM older than 12 cal kyr BP (Metcalfe et al., 2015), we do not rule out that during the onset of MIS3, a relatively warm period (Bradley and Diaz, 2021), mechanisms responsible for moisture transport towards northern Mexico from the Caribbean were similar to today, when higher atmospheric temperatures promote a greater entry of humidity to the Petén area between July and September (Hu and Dominguez, 2015).

~~The TOC/TN ratio has been used as an indicator for the source of organic matter in lacustrine sediment sequences (Talbot and Johannessen, 1992; Meyers and Ishiwatari, 1995). During the interval 59-53 cal ka BP, low TOC/TN ratios (mean 10.7±3.2) indicate that the sediment organic matter was predominantly of aquatic origin (Meyers et al., 2003). This is consistent with the pollen-based inference for extensive grasslands around Lake Petén Itzá, indicating that there was relatively little terrestrial biomass in the watershed that could have contributed to the lake sediments (Bush et al., 2009). The absence of arboreal vegetation, visible in the largest deposit of aquatic organic matter in our record, with~~

Con formato: Color de fuente: Automático

Con formato: Color de fuente: Automático

Con formato: Color de fuente: Automático, Subíndice

Con formato: Color de fuente: Automático

Con formato: Color de fuente: Automático

the simultaneous increase in lake levels have been associated with winter rains from north cold fronts (Hodell et al., 2008). This has previously been linked to the expansion of the Laurentide Ice Sheet, bringing winter rains into Central America, producing drier summers given the high seasonality (Bradbury, 1997).

Mn/Fe ratios are used to infer variations in redox conditions in lakes (Wersin et al., 1991; Naeher et al., 2013; Friedrich et al., 2014; Ortega-Guerrero et al., 2020). Lower values of Mn/Fe generally indicate low concentration of O_2 in the water column, that is explained by a more rapid reduction of Mn than Fe under anoxic conditions favoring the preferential Mn deposition. Whereas, higher values of Mn/Fe suggest high levels of O_2, as Fe oxidizes quicker than Mn under an oxic environment. During this unit, low values of the Mn/Fe ratio (mean 3.7±0.3) in the sediments indicate anoxic conditions in the bottom waters of Lake Petén Itzá. Anoxia may have been associated with high water level as today, which prevented the wind-driven mixing of the water column.

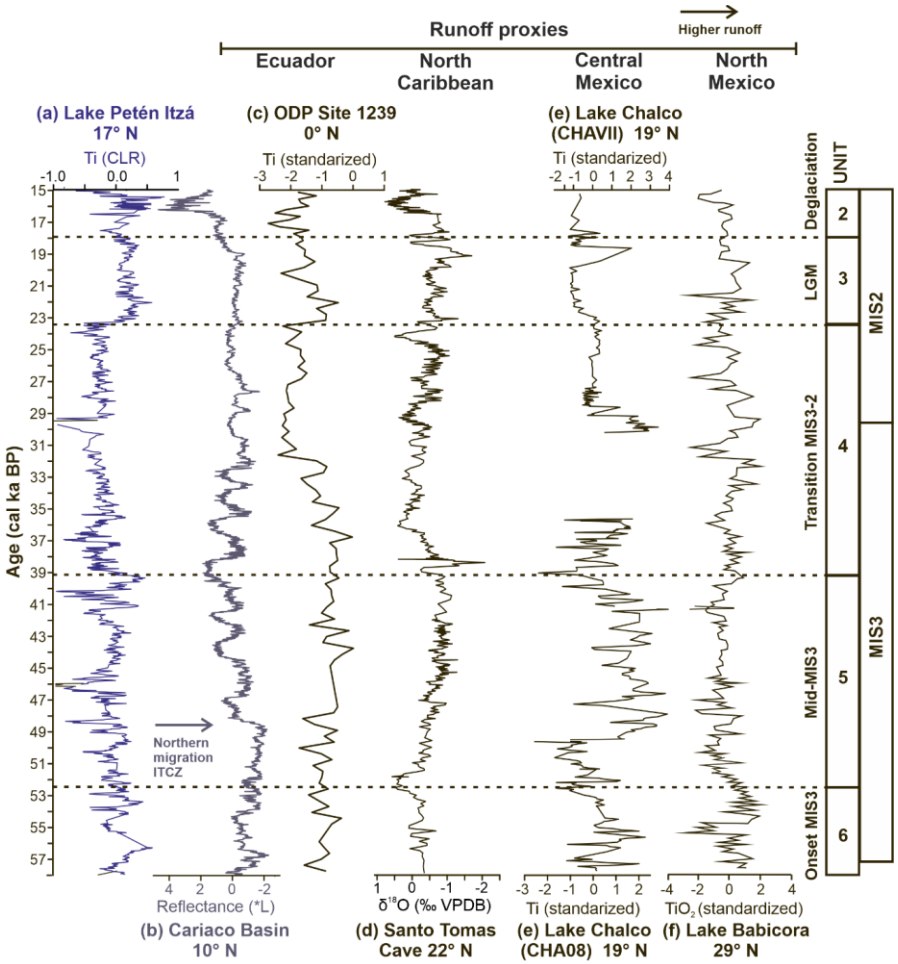

Figure 45. Comparison of paleoclimate and runoff/precipitation records spanning MIS3-2. The records are arranged in latitudinal South-North order. Aa) Centered log-ratio Ti record from Lake Petén Itzá (this study). b) Reflectance data from the core MD03-2621, of the Cariaco Basin (Deplazes et al., 2013). c) Standardized record of Ti obtained from the IODP Site 1239 site in the equatorial Pacific Ocean (Rincón-Martinez et al., 2010). B) Reflectance data from the core MD03-2621 of the Cariaco Basin (Deplazes et al., 2013). C) Calibrated record of Ti from Lake Petén Itzá (This study). Dd) $\delta^{18}O$ data from a stalagmite from Larga CaveSanto Tomas Cave, Puerto RicoCuba (Warken et al., 20201919). Ee) Standardized record of Ti from in two sedimentaryary sequences fromof Lake Chalco, Central Mexico (CHAVII site obtained from Lozano-García et al., 2015. CHA08 site from Martínez-Abarca et al., 2021b). Fg) Standardized TiO_2 data obtained from Lake Babicora, nNorthern Mexico (Roy et al., 2013). Reflectance data from the core MD03-2621 of the Cariaco Basin (Deplazes et al., 2013). Original data were standardized by subtracting the mean of the data and dividing by the standard deviation. G) Numerical estimate of summer precipitation (June/July/August) made with data from Lake Tulane, Florida (Donders et al., 2011). Background colouring indicates the dominance

Con formato: Justificado, Interlineado: 1.5 líneas

~~of wet (blue) or dry (red) conditions among the records. Similarly, the preferential position of the Intertropical Convergence Zone (ITCZ) through the record is indicated. The six lithological units of the Petén Itzá record, as well as the MIS3-2 periods, are encapsulated by rectangles on the right.~~

5.1.2 Mid-MIS3 ~~Unit 5~~ (52.7-39.3 cal ka BP): ~~A s~~Shift to higher evaporation and lower ~~water~~ lake levels ~~during the mid-MIS3~~

The mid-section of MIS3 corresponds to Unit 5. High Ti ~~Ti log-ratio values~~ (mean ~~-2~~0.1±0.~~6~~3) and stable quartz contents (mean 3.2±2.0%) indicate that precipitation and runoff to Lake Petén Itzá remained high ~~high~~ during the deposition of Unit 5 but they were lower than in Unit 6 (Fig. 3). ~~This is also apparent from the relatively invariant quartz content (mean 3.2±2.0%), which support the inference for high precipitation and chemical weathering. Unit 5 is characterized by a pronounced~~An increase in TOC content (mean 2.8±1.0%) at 51 cal ka BP indicates increased productivity, and a pronounced increase in TOC/TN ratios (mean 18.7±5.9), indicates~~ing~~ a higher loading of terrestrial organic matter to the lake~~deposition of an admixture of aquatic and terrestrial organic matter~~ (Meyers et al., 2003). The TOC content reaches maxima in two intervals, around 46.2 and 40.2 cal ka BP, coinciding with increased evaporation (Ca/(Ti+Fe) ratios of up to 5.9). These two periods correlate with peaks of oxic conditions, as suggested by maxima of the Mn/Fe ratio (0.2 and -1.6; Fig. 3). Our data thus suggest more oxygenated bottom waters, possibly associated with lower lake-levels, which resulted in greater wind-induced mixing of the water column (Yu et al., 1984; Gale et al., 2006). A short-lived increase in runoff terminates Unit 5, a result of more humid conditions that may have delivered greater nutrient loads to the lake. The latter would have favored the input of aquatic organic matter to the sediments between 40.4 and 39.3 cal ka BP. Wetter conditions and greater autochthonous production are supported by high Ti (up to 0.7) and low TOC/TN ratios (6.7), respectively.

A decrease in runoff and lake-level lowering, which interrupted the general wet climate during mid-MIS3, was also inferred by Pérez et al. (2021) from Site PI-6 based on ostracod assemblages that reflect higher conductivity. This was explained by an increase in ion concentrations in the water column associated with a higher evaporation/precipitation ratio. In addition, the presence of the high conductivity-preferring diatom *Cyclotella petenensis* was reported from Site PI-6 sediments during between 40 and 39 cal ka BP (Paillès et al., 2018), suggesting high evaporation rates. Enhanced evaporation was associated with an increase contribution of terrestrial organic matter. This may at first appear contradictory. However, it is consistent with pollen-based observation of an increase in non-arboreal communities, e.g., Poaceae during Unit 5 at Site PI-6 (Fig. 4; Correa-Metrio et al., 2012). We interpret the increase in terrestrial organic matter to not reflect changes in the terrestrial vegetation, but rather the proximity of the plant communities (grasslands) to Sites PI-2 and PI-6, because of the shrinking of lake surface area. This was observed at Lake Tzibaná (southern Mexico) during a 20-m decline in lake level, during which vegetation colonized subaerially exposed lake bottom and large amounts of organic matter entered the remnant basin during sporadic periods of rain (Martínez-Abarca et al., 2022).

Con formato: Color de fuente: Automático

Con formato: Color de fuente: Automático

~~, while the increase in TOC content (mean 2.8±1.0%) indicates increased productivity and more reducing conditions in the lake. The increased relative contribution of terrestrial organic matter to the sediment is consistent with the pollen-based inference for the increase of arboreal communities such as Quercus and Pinus during Unit 5 (Correa-Metrio et al., 2012).~~ Whereas our Lake Petén Itzá record~~data~~, together with other lake and speleothem archives~~records~~ from the circum-Caribbean and Gulf of Mexico, such as~~(e.g.~~ Lake Tulane, Florida (Grimm et al., 2006); Abaco Island, Bahamas (Arienzo et al., 2017); Santo Tomas Cave, Cuba (Warken et al., 2019) and Larga Cave, Puerto Rico (Warken et al., 2020), reveal moderately wet conditions, several paleoclimate records from northern and c~~North and C~~entral Mexico, including those ~~such as those~~ from Lakes Babicora (Roy et al., 2013), Tecocomulco (Caballero et al., 1999), Patzcuaro (Bradbury, 2000) and Chalco (Ortega-Guerrero et al., 2020), indicate reduced rainfall ~~at that time~~during the midst of MIS3 (Fig. 5). This spatial climate~~climatic~~ contrast may have been associated with the beginning of the southward migration of the ITCZ. The ΔSST between the eastern Pacific and the Caribbean shows a slight decrease, suggesting that the CLLJ decreased in intensity (Fig. 6), thereby promoting low runoff into Lake Petén Itzá.~~the position of the ITCZ over the Caribbean region and the equatorial zone.~~ Despite this, climate at Petén Itzá remained relatively humid, possibly attributed to moisture supply associated with a stronger AMOC. ~~The dominance of wetter conditions in records from the Caribbean, Gulf of Mexico and Florida may suggest that moisture supply may be associated with the AMOC, since i~~Indeed, it~~t~~ has been shown that a~~the~~ strengthening of the AMOC may promote~~s~~ an enhanced northward heat transport, a lower cross-equatorial ΔSST~~sea-surface temperature gradient~~ and, ~~in consequence~~consequently, wetter conditions in the tropical Northern Hemisphere (Fig. 7; Clark et al., 2001; Waelbroeck et al., 2018). ~~However, more modeling studies would be required to evaluate the climatic drivers consistent with data from the whole region to address this question around regional differences during the middle of MIS3.~~

~~A gradual increase in the Mn/Fe ratios suggests oxygen enrichment in the lake bottom waters during Unit 5. Particularly, two peaks of oxia are presented around 46.1 and 40.3 cal ka BP (maxima of ~1.3 and ~2.1 respectively; Fig. 3). Those intervals were associated with high evaporation rates, inferred from an increase in the Ca/Ti+Al+Fe ratio (up to 5.6). Our data thus suggest more oxygenated bottom waters possibly associated with a lowering of water level that resulted from greater wind-induced mixing of the water column (Yu et al., 1984; Gale et al., 2006). Increased mixing may be also associated with a reduction in the lake-surface temperature causing less stratification (e.g. Caballero and Vazquez, 2020); however, our data are not able to infer these temperature changes. These intervals of lower water level in Lake Petén Itzá were inferred previously by Pérez et al., (2021) as times of higher conductivity based on ostracod analysis. This was related to the relative increase in the concentrations of cations and anions in the water column associated with higher evaporation. In addition, the presence of the high conductivity-preferring diatom *Cyclotella petenensis* has been reported in sediments of Site PI-6 during this period (Paillès et al., 2018) and suggests a high evaporation rate. Unit 5 terminates with a short increase in runoff, as a result of more humid conditions, and aquatic organic matter input between 40.4 and 39.3 cal ka BP, as indicated by high Ti (up to ~1.3) and low TOC/TN ratios (6.7).~~

Con formato: Color de fuente: Automático

Con formato: Color de fuente: Automático

Con formato: Color de fuente: Automático

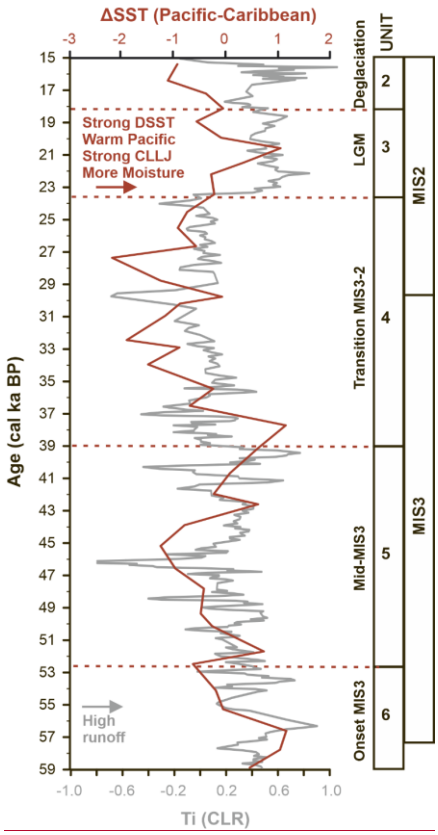

Figure 6. Low-frequent co-variability between runoff (Ti) and changes in the intensity of the Caribbean Low-Level Jet (CLLJ). As a proxy for the CLLJ, we use the Pacific-Caribbean differences in sea surface temperature (ΔSST). A stronger ΔSST due to a cooling in the Caribbean and/or warming in the Pacific cause a stronger CLLJ with more precipitation and runoff at Lake Petén Itzá. Red line: ΔSST calculated by subtracting annual SST values from marine sediment record at Site MD02-2529 in the eastern Pacific (Costa Rica; Leduc et al., 2007) from values at ODP Site 999A located in the Caribbean (Schmidt et al., 2006). Site 999A SST data were obtained using Mg/Ca ratios of the planktonic foraminifera *Globigerinoides ruber*, whereas the MD02-2529 dataset is based on the $U^{K'}_{37}$. As both records contain different temporal resolution, we approximated the closest ages between both records and subtracted the available SST data. Grey line: Ti from Site PI-2 in Lake Petén Itzá (this study). Ti data were averaged using a LOESS smoothing function (factor=10). The different time periods discussed in the text, are linked to the stratigraphic units defined by Mueller et al. (2010).

5.1.3 Transition MIS3-2 ~~Unit 4~~ (39.3-23.5 cal ka BP): Great hydrological instability ~~during the final stage of MIS3 and onset of MIS2~~

Con formato: Color de fuente: Automático

Con formato: Color de fuente: Automático, Superíndice

Con formato: Color de fuente: Automático

Con formato: Color de fuente: Automático, Subíndice

Con formato: Color de fuente: Automático

The final stage of MIS3 and the beginning of MIS2 correspond to Unit 4. This unit is~~Unit 4 corresponds to the transition into the final stage of MIS3 and the beginning of MIS2. It is~~ characterized by ~~great~~ high variability in ~~the hydrological proxies~~runoff and evaporation. The decrease in Ti (mean -0.3±0.3) ~~A general and significant trend of reduced Ti content (mean -2.6±0.6)~~ indicates a ~~decrease~~ decline in runoff. Moreover, variable but higher Ca/(Ti~~+Al~~+Fe) ratios ~~ratios~~ (mean 3.4~~6~~±0.7) indicate~~s~~ an increase in evaporation relative to Unit 5 (Fig. 3). In addition, ~~$CaCO_3$~~ the carbonate content ~~obtained by XRD~~ shows a trend similar ~~trend~~ to that of the Ti ~~log ratio~~ dataset. This coupling may suggest an input of detrital carbonate from ~~be response of~~ the karstic bedrock ~~composition~~ in the catchment ~~area~~. Carbonate in lake sediments ~~Although the entry of $CaCO_3$ into the lakes~~ is commonly related to: 1) inorganic calcite precipitation and consequently to periods of high productivity and/or evaporation, and 2) high nutrients input ~~organic production that~~ promotinge~~s~~ eutrophication, an increase in pH and, ~~in consequence~~consequently, enhanced biogenic calcite formation~~$CaCO_3$~~ (Megard, 1993; Dean, 1999). Mineralogical data display higher values of gypsum (mean 53.9±3.4%), suggesting drier conditions and hence lower chemical weathering in the catchment.~~,~~ High and stable values of the Mn/Fe ratio (mean -3.3±0.5) indicates oxic bottom waters within this unit, possibly associated with a decline in lake level and greater wind mixing. TOC/TN ratios rapidly increase to values >20, suggesting a relative decline in the contribution of aquatic organic matter input relative to that from terrestrial sources. After 32 cal ka BP, however, TOC/TN ratios decreased gradually to values of ~10, indicating a shift to again a dominance of ~~higher~~ aquatic ~~and lower terrestrial~~ organic matter ~~input~~. In addition, lower TOC values (mean 1.9%±1.0) in Unit 4 may suggest a low preservation of sedimentary organic matter as a result of its oxidation favored by the establishment of the epilimnion at the PI-2 site, the latter as result of the decline in lake levels.

~~it is possible that during Unit 6 the variability of carbonate deposition in the sediments is associated with the input of detrital carbonate minerals derived from carbonate rocks in the catchment basin. Mineralogical data display higher values of gypsum (mean 53.9±3.4%), suggesting drier conditions and hence lower chemical weathering in the catchment. Stable but high contemporaneous values of Mn/Fe ratios (mean -3.3±0.4) indicates oxic bottom waters along this unit, possibly associated with a decline in water level and greater wind mixing.~~ Lower lake levels during the MIS3-2 transition were ~~also~~ inferred previously using the~~in~~ SSite PI-6 core (~~by~~ Cohuo et al., ~~(~~2020~~;) and~~ Pérez et al., ~~(~~2021), from an increase in the relative abundance of the endemic ostracod *Paracythereis opesta*, a benthic species associated with shallow-water environments (<40 m depth) (Cohuo et al., 2017; Echeverría et al., 2019). In addition, Paillès et al.~~,~~ (2018) found abundant ~~diatoms belonging to~~ *Cyclotella petenensis* and *C. cassandrae*~~,~~ in deposits from that Unit in PI-6. These diatom species are ~~both~~ characteristic ~~for a~~of high-conductivity ~~environment~~waters, which agrees with our interpretation. ~~Shallow~~ Lower ~~lake~~ water level~~s~~ that enabled oxygenation of the water column ~~and the epilimnion establishment in the site~~ is also supported by high $\delta^{13}C$ values ~~-~~measured in the ostracod *Lymnocythere opesta* at Site PI-6~~at Site PI-6~~ (Fig. 4; Escobar et al., 2012). The gradual decrease in runoff, associated with dry conditions at site PI-2, correlates with a decrease in magnetic susceptibly at Site PI-6 (Fig. 4). By other hand, the high proportions of terrestrial organic matter prior to 32 cal ka BP coincide with an increase in sedimentary $\delta^{13}C_{TOC}$ values in the PI-6 record, which was interpreted to reflect a greater proportion of C_4 plants in the catchment, indicative of drier climate (Mays et al., 2017). The contribution of allochthonous organic matter may also have decreased because of the spread of C_4 savanna vegetation in the lake catchment, with high relative abundances of Cyperaceae and Poaceae (Fig. 4; Correa-Metrio et al., 2012).

Con formato: Color de fuente: Automático

Con formato: Color de fuente: Automático

~~Otherwise, increases in evaporation inferred from Ca/Ti+Al+Fe data simultaneous with increases in Mn/Fe ratio (bottom oxia) correlate with periods of decrease in lake volume and site exposure to the epilimnion around 37.1 and 29.6 cal ka BP. Whereas, increases in runoff at Site PI-2 correlate with an increase in lake volume and bottom anoxia at Site PI-6. Contemporaneously, contrary~~Paleoclimatic conditions different from ~~to~~ those around~~present in~~ Lake Petén Itzá ~~have~~ were inferred from ~~been reconstructed at~~ lakes of central and northern Mexico, where a wetter climate and less saline conditions prevailed (e.g. Lake Babicora, Chávez-Lara et al., 2012; Lake Chalco, Caballero et al., 2019; Fig. 5~~4~~). Additionally, in more northerly records from the Gulf of Mexico, a gradual reduction in humidity was~~is~~ also inferred ~~reconstructed during~~for the time period when~~deposition of~~ Unit 4 was deposited, using ~~by~~ paleo-precipitation models ~~from Lake Tulane (Florida, USA)~~ (Donders et al., 2011). This inter-regional comparison of paleoclimati~~c~~e records indicates that the Petén ~~Itzá~~ region and northern Gulf of Mexico were dominated by dry conditions during the ~~end of~~ MIS3-2 transition. We suggest that during the transition (39.3-23.5 cal ka BP), the ITCZ was mainly located farther south, accounting for the lower precipitation and consequent reduction in runoff to Petén Itzá. The gradual trend towards drier conditions observed after 29 cal ka BP, however, resembles the trend of reduced SST in the eastern Pacific that may have lessened the intensity of the CLLJ, resulting in decreased moisture transport to the Petén region. Therefore, it is possible that much of the runoff to Lake Petén Itzá depended on the position of the CLLJ during the transition.

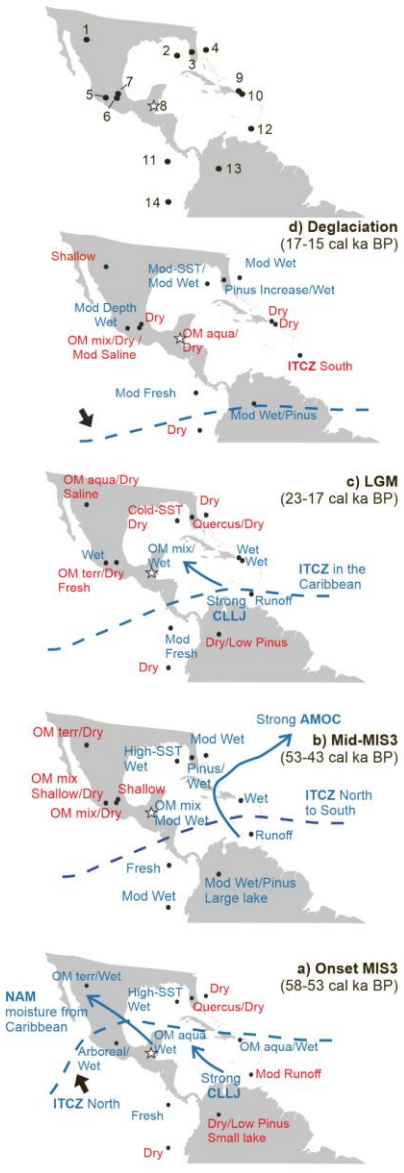

Figure 7. ~~MGeographic m~~aps showing regional paleoclimati~~c~~e records and limnological/climat~~eic~~ characteristics inferred for the ~~onset of~~ (a) o~~O~~nset of MIS3, (b) mid-MIS3, (c) the Last Glacial Maximum (LGM) and (d) deglaciation. B~~The b~~lue ~~colors~~ refers to ~~reconstructed~~ mainly humid conditions, ~~while~~ whereas~~the~~ red ~~color i~~ndicates primarily dry conditions. Possible mechanisms providing moisture to the northern Neotropics are indicated. Abbreviations: OM aqua (aquatic organic matter), OM terr (terrestrial organic matter), OM mix (mixed organic matter), Mod (moderate), SST (s~~S~~ea s~~S~~urface t~~T~~emperature), AMOC (Atlantic Meridional Overturning Circulation), ITCZ (Intertropical Convergence Zone), CLLJ (Caribbean Low-Level Jet). Sites: 1) Lake Babicora (Roy et al., 2013), 2) marine record MD02-2575 (Ziegler et al., 2008), 3) Lake Tulane (Grimm et al., 2006), 4) Bahamian speleothem record AB-DC (Arienzo et al., 2017), 5) Lake Patzcuaro (Bradbury ~~et al.~~,

Con formato: Color de fuente: Automático

Con formato: Color de fuente: Automático

2000), 6) Lake Chalco (Martínez-Abarca et al., 2021b), 7) Lake Tecocomulco (Caballero et al., 1999), 8) Lake Petén Itzá (this study, marked with a star), 9) Blanchard Cave (Royer et al., 2017), 10) Larga Cave (Warken et al., 2020), 11) marine record MD02-2529 (Leduc et al., 2007), 12) Cariaco Basin record MD03-2621 (Deplazes et al., 2013), 13) Lake Fúquene (Groot et al., 2011), 14) marine record ODP Site 1239 (Rincón-Martínez et al., 2010).

5.1.4 Last Glacial Maximum ~~Unit 3~~ (23.5-18.0 cal ka BP): A sudden large increase in runoff ~~during the Last Glacial Maximum~~

The Last Glacial Maximum (LGM) corresponds to Unit 3~~Unit 3 corresponds to the Last Glacial Maximum (LGM)~~, which ~~has been~~was studied previously using sediments from ~~Site~~ Site PI-6 ~~in Lake Petén Itzá~~ (Hodell et al., 2008; Bush et al., 2009; Pérez et al., 2011; Mays et al., 2017). Ti ~~values are~~ is highest in Unit 3 and ~~oscillate~~ varies between ~~-0.6 and-~~ 1.1, showing an ~~indicative of an~~ abrupt increase in humidity and runoff (Fig. 3). This is also supported by ~~T~~the increases in clay and quartz contents (means of 8.5±2.9% and 5.1±2.5%, respectively). ~~indicates an increase in humidity (Van De Kamp, 2010).~~ Ca/(Ti+~~Al+~~Fe) ratios were~~ratios were~~ lowest in this unit (mean ~~-~~1.~~7~~9±0.4~~5~~), indicating significantly reduced rates of evaporation (Fig. 3). TOC/TN ratios <10 ~~during the LGM~~ suggest ~~a~~ high ~~loading~~ sedimentation of aquatic-derived organic matter ~~to the sediments~~. ~~An average reduction in~~ Lower~~the~~ Mn/Fe ratios ~~ratios~~ (mean -3.7±0.~~2~~3) and generally higher TOC content (2.2±0.6%) suggest that the deep lake was characterized by persistent bottom water anoxia that facilitated the preservation of organic matter. ~~c conditions, likely associated with higher water levels.~~

More humid~~Wetter~~ conditions and higher lake levels during the deposition of Unit 3 were also inferred from ~~recognized in~~ sediments ~~of~~ at S~~S~~ite PI-6. High magnetic susceptibility and density values suggest high detrital input (Fig. 4; Hodell et al., 2006, 2008), while more negative $\delta^{18}O$ and $\delta^{13}C$ values of ostracod shells indicate higher lake levels and ~~the~~

establishment of an anoxic hypolimnion at ~~Site~~ Site PI-6 (Escobar et al., 2012; Pérez et al., 2013). Ostracod assemblage analysis revealed the presence of deep-water species (>40 m depth) such as *Cypria petenensis* (Pérez et al., 2021), ~~while~~ while the presence of the diatom *Discotella gabinii* indicates ~~diatom data indicates~~ low-conductivity and alkaline water during the LGM ~~based on the presence of *Discotella gabinii*~~ (Paillès et al., 2018).

W~~In addition, w~~et conditions during the LGM were also ~~inferred~~ deduced ~~using~~ from ~~oxygen stable isotope ($\delta^{18}O$)~~ values in ~~measurements in~~ speleothems from the Caribbean region, including those from Blanchard Cave, Guadaloupe (Royer et al., 2017), Larga Cave, Puerto Rico (Warken et al., 2020), Santo Tomas Cave, Cuba (Warken et al. 2019) and Juxtlahuaca Cave, Guerrero, southwest Mexico (Lachniet et al., 2014). In contrast, dry conditions were inferred~~deduced~~ from other ~~multi-proxy~~ paleoclimate records from central and northern Mexico (e.g. La Piscina de Yuriria [~~(~~Davies, 1995~~)~~]; Lake Patzcuaro [~~(~~Bradbury, 2000~~)~~]; Lake Babicora [~~(~~Roy et al., 2013~~)~~]; and Lake Chalco ~~(~~[Lozano-García et al., 2015~~)~~]), the northern Gulf of Mexico (e.g. Lake Tulane, Florida [~~(~~Grimm et al., 2006; Donders et al., 2011~~)~~]), Colombia (Lake Fúquene, Groot et al., 2011, 2013; Vriend et al., 2012) and the East Equatorial Pacific ODP-1239 record (Rincón-Martínez et al., 2010) (Fig. 5). This is consistent with the multi-record analyses of ~~corresponds with the~~ Bradbury (1997) and Ramírez-Barahona and Eguiarte (2013), which ~~multi-record analyses, which~~ showed dry conditions for~~in~~ western central Mexico and concomitantly wet conditions in eastern and southern Mexico~~the east~~. ~~The trend observed in o~~Our regional comparison using ~~with other available~~ records from Mexico, the Gulf of Mexico, and the Caribbean indicates that the ITCZ may have been ~~restricted~~ mainly positioned over ~~to~~ Central America during the LGM (Fig. ~~5~~7). It is also possible that the decrease in atmospheric temperatures reduced the amount of humidity that entered Mexico from the Caribbean (Hu and Dominguez, 2015). Previous studies showed that during the LGM, an analog to the negative phase of the El Niño Southern Oscillation (ENSO) persisted, which resulted in a weakening of the NAM, explaining the droughts in central and northern Mexico (Lachniet et al., 2013). The ΔSST suggest that water temperatures in the eastern Pacific were ~1 °C higher than those in the Caribbean during the LGM (Fig. 6), which may have promoted a more intense CLLJ and thus increased moisture transport to the Caribbean, including to the Petén region. This is consistent with estimates from fossil records (e.g. Trend-Staid and Prell, 2002; Kucera et al., 2005) and numerical simulations (e.g. Kitoh and Murakami, 2002; Otto-Bliesner et al., 2009). ~~However, future numerical approach may provide more information in the reconstruction of atmospheric processes during the LGM in the Northern Neotropics.~~

5.1.5 Deglaciation ~~Unit 2~~ (18.0-15.0 cal ka BP): Low runoff and enhanced evaporation ~~during the deglaciation~~

At the onset of Unit 2 (18.0-16.3 cal ka BP), a decrease in Ti ~~values~~ to ~~4.9~~0.1 and an increase in Ca/(Ti~~+Al~~+Fe) ratios ~~ratios~~ and gypsum content (averages of 3.~~2~~3±1.4 and 78.2±32.8%, respectively) indicate a ~~decrease~~ reduced ~~in~~ runoff, drier conditions and an increase in evaporation~~, rate~~ which would have ~~decreased the~~resulted in lower lake ~~water~~ level (Fig. 3). As in Unit 4, ~~$CaCO_3$~~ carbonate and Ti values~~-~~ are coupled ~~with the Ti data trend in Unit 2~~, indicating that input of carbonates into the lake may depend partly on runoff and precipitation. This is consistent with ostracod-based inferences from ~~in S~~Site PI-6 that indicate lower water levels and greater conductivity ~~in Lake Petén Itzá~~ with a dominance of littoral ostracod species such as *Cypridopsis vidua*, *Heterocypris putei* and *Paracythereis opesta* (Díaz

et al., 2017; Cohuo et al., 2018; Pérez et al., 2021). ~~Similarly~~Likewise, high $\delta^{18}O$ values in ~~of both~~ ostracod shells~~s~~ and gypsum hydration water indicate high evaporation (Escobar et al., 2012; Hodell et al., 2012; Grauel et al., 2016). An estimated 56-m lake level decline was ~~decline has been~~ reported by Anselmetti et al. (2006) and Hodell et al.~~,~~ (2006), based on the occurrence of a paleo~~-~~shoreline in seismic ~~images~~profiles. ~~corresponding to this unit.~~ Comparatively low TOC/TN ratios at Site PI-2 (mean 11.5±4.8) indicate a decrease in the relative contribution of organic matter from terrestrial sources. Furthermore, *n*-a~~A~~lkane distributions in the PI-6 record show a reduced loading of ~~predominance of~~ terrestrial plant material between 18 and 16 cal ka BP~~in Unit 2~~ (Mays et al., 2017). ~~Based on pollen analysis, t~~This may be explained dy the predominance of grassland ~~e vegetation cover~~ in the vicinity of the lake ~~was largely composed of grassland~~ (Fig. 4; Bush et al., 2009), which may have ~~probably~~ contributed little to the sedimentary organic matter~~. , as indicated by low TOC values in Unit 2 (mean 0.7±0.4%).~~

Dry climate conditions such as at Petén Itzá were~~have been~~ deduced from lake sediments ~~deposits~~ in lakes of central Mexico and the Caribbean (Bradbury, 2000; Lozano-García et al., 2015; Royer et al., 2017; Caballero et al., 2019; Martínez-Abarca et al., 2019; Warken et al., 2020), whereas records from the northern Gulf of Mexico suggest wet conditions that originated from extra-tropical fronts that moved south during the early phase of deglaciation ~~at the same time~~ (Ziegler et al., 2008; Donders et al., 2011; Roy et al., 2013; Arienzo et al., 2017). This can be explained by the latitudinal migration ~~to the south~~ of the ITCZ to the south after the ~~relative to~~ LGM and the collapse of the ~~caused by the~~ AMOC ~~collapse~~ during HS1, which ~~that~~ promoted dry environments throughout Central Mexico and the Caribbean (Fig. ~~5~~7). ~~It is possible that factors such as cold fronts will add moisture to the northernmost records of Mexico and the Gulf of Mexico.~~

Unit 2 terminates with a sudden increase in Ti ~~values~~ (up to ~~-1.3~~0.8) between 16.3 and 15.0 cal ka BP, indicating an increase in precipitation and runoff. A decrease in Ca/(Ti~~+Al~~+Fe) (up to -0.1) suggests evaporation remained low, and low ~~values of~~ TOC/TN ratios (~~<up to~~ 10.9) indicate~~s~~ a predominance ~~aquatic~~of aquatic organic matter. ~~dominated the sediment. This suggests that A~~although dry conditions may have prevailed at the beginning of the deglaciation corresponding to the first ~~with a first~~ stage of HS1, the second part (17-15 cal ka BP) was characterized by ~~had~~ an increase in runoff and precipitation (Hodell et al., 2012; Pérez et al., 2013). This may have been ~~most likely~~ linked to a slight AMOC recovery that precede~~d~~ the ~~a~~ second stage of HS1, indicated by lower values of $\delta^{18}O$ foraminifera tests in the North Atlantic (McManus et al. 2004). ~~in Petén Itzá (McManus et al., 2004; Hodell et al., 2012; Pérez et al. 2013).~~

Con formato: Color de fuente: Automático

5.2 Millennial-scale climate ~~climate associated with hydrological~~ variability~~changes in Lake Petén Itzá~~

Whereas long-term transient climate changes have been inferred from multiple records in the region, our high-resolution geochemical records from Site PI-2 also reveal short-term variations, including abrupt shifts in hydrological proxies between 59 and 15 cal ka BP, similar to those observed in the GICC05 ice-core record from Greenland (Svensson et al., 2008). Low Ca/(Ti+Fe) ratios are associated with high Ti during GI. This suggests wet conditions and enhanced runoff. Maxima of Ca/(Ti+Fe) and increased gypsum content at Site PI-2 are largely contemporaneous with increases in the *L reflectance values in marine core MD03-2621 from the Cariaco Basin, offshore Venezuela (Fig. 8), particularly during GS11-2 (Peterson et al., 2000; Deplazes et al., 2013). Transport of moisture to the Petén

region between 42 and 24 cal ka BP seems to have been dominated by changes in SSTs between the eastern Pacific and the Caribbean, and in turn, by the intensity of the CLLJ. However, variability in runoff and evaporation, suggested by our Ca/(Ti+Fe) ratios during GS11-2 and in the Cariaco L* reflectance record, may have been largely influenced by millennial-scale changes in the position of the ITCZ.

Maxima in Ca/(Ti+Fe) and hence more humid conditions are more frequent during GS11-2. Consequently, the intensity of evaporation (dry conditions) was more pronounced between 42 and 32 cal ka BP, suggesting that the Lake Petén Itzá basin was more susceptible to changes in precipitation, evaporation and drainage during the middle and end of MIS3. No apparent increases in Ca/(Ti+Fe) were observed during GS14-12. However, the Petén Itzá chronology has a ±2 kyr uncertainty for ages >45 cal ka BP and we therefore cannot exclude the possibility that the Ca/(Ti+Fe) increases at 48.4, 46.2 and 43.8 cal ka BP correspond to low values of *L reflectance in the Cariaco Basin record at 49.3 (GS14), 48.1 (GS13) and 43.7 (GS12) cal ka BP, respectively.

The high resolution of the geochemical data, together with the high sedimentation rates at Site PI-2 compared to PI-6, enabled us to study the impact of several GS on the northern Neotropics (Fig. 8). GS 11 and 10 show a gradual increase in evaporation over ~1200 years, followed by a rapid decrease over ~400 years. On the contrary, GS9-6 started with a rapid increase in evaporation over ~500 years that was followed by a gradual reduction in evaporation over ~1200 years. This difference may likely be explained by changes in the intensity of the CLLJ. During GS 11 and 10, the CLLJ was stronger and provided more moisture to the region (Fig. 6). Consequently, millennial scale oscillations in the position of the ITCZ and particularly its displacement to the south were possibly muted by the CLLJ. With respect to GS9-6, the intensity of the CLLJ and its capacity to transport moisture decreased, so any millennial-scale change in the ITCZ produced abrupt changes in lake evaporation and catchment runoff. Ca/(Ti+Fe) maxima associated with GS5-3 are less pronounced, which may have been a consequence of a weaker CLLJ during the onset of MIS2 as high values of ΔSST between the Caribbean and Eastern Pacific reveal between 34 and 24 cal ka BP. Evidence of GS2 is missing and may be linked to the onset of the LGM which was characterized by high humidity in Petén (see section 5.1.4) and may have suppressed the GS2 signal in the sediment record.

The response to GI and GS in Lake Petén Itzá has been studied in sediments from Site PI-6. For example, Correa-Metrio et al. (2012) provided a high-resolution record of pollen and carbonized material (~200 year-resolution), which revealed an increase in forest fires in this region during GS. This is consistent with high evaporation in response to dry conditions in the northern Neotropics. The latter is more apparent for GS13, GS9 and GS5, whose presence in our record is synchronous with the North Atlantic IRD deposits associated with HS5-3, respectively. The enhanced Ca/(Ti+Fe) ratios during GS13, GS9 and GS5 in Lake Petén Itzá may have been a response to dry conditions that dominated during HS. In addition, higher abundances of gypsum were found during GS13 and GS9, suggesting high evaporation of lake water (Fig. 8). Similar increases in Ca/(Ti+Fe) and gypsum content are observed during GS8, GS7, GS5, GS4 and GS3. We did not notice an increase in gypsum content during GS11, GS10 and GS6, which may be related to the low sampling resolution in this interval. The higher Ca/(Ti+Fe) ratios, however, points to an increase in evaporation.

Con formato: Color de fuente: Automático

Sediments from Petén Itzá Site PI-6 reveal short-term variations in lithology and in several proxies such as stable isotopes, pollen and charcoal, which have been related previously to millennial climate oscillations in Greenland and the adjacent North Atlantic, such as GI, GS and HS during MIS3-2 (Hodell et al., 2008; Correa-Metrio et al., 2012; Escobar et al., 2012). Our geochemical record from Site PI-2 supports with the association of millennial variations in Petén hydroclimate and the short-term oscillations observed in records such as the GICC05 ice core in Greenland and the marine core MD03-2621 in the Cariaco Basin, offshore Venezuela (Fig. 6). Ti data from the Petén Itzá record indicate distinct episodes of elevated runoff throughout the record, which largely correlate with the warm episodes GI14-2 recorded in the $\delta^{18}O$ values from the GICC05 ice core between 59 and 15 cal ka BP (Svensson et al., 2008). The presence of Ti maxima and increased clay content in Site PI-2 is largely contemporaneous with decreases in reflectance values on marine core MD03-2621, particularly within GI11-2 (Peterson et al., 2000; Deplazes et al., 2013). This indicates that the high runoff in Petén Itzá during GI was associated with the northern migration of the ITCZ inferred from the Cariaco Basin. All GI are characterized by green, clayey mud and clay-calcite silt deposits as described previously by Mueller et al., (2010) and discernible in images of the PI-2 cores (Fig. 7). The intensity of Ti maxima associated with GI11-2, and consequently the intensity of runoff, is greater in sediments older than 35 cal ka BP, suggesting that the Lake Petén Itzá basin was more susceptible to changes in precipitation and drainage during MIS3. After 35 cal ka BP, Ti maxima associated with GI are less pronounced, which may be a consequence of the more southerly average position of the ITCZ during MIS2. On the contrary, there are no clear increases in Ti values associated with the northern migration of the ITCZ during GI14-12. However, the Petén Itzá chronology has a ±2 kyr uncertainty mostly for ages >45 cal ka BP. Therefore, together with the still discussed Greenland chronology/uncertainties for ages >42 cal ka BP (Svensson et al., 2008), we cannot exclude the possibility that the Ti increase and Ca/Ti+Al+Fe decline at 51.5, 46.8 and 45.7 cal ka BP correspond to the increments presented in the Cariaco Basin record at 53.8 (GI14), 49.3 (GI13) and 46.0 (GI12) cal ka BP, respectively.

The Ca/Ti+Al+Fe data show a series of peaks contemporaneous with decreases in Greenland $\delta^{18}O$ values associated with the cold periods of GS (Fig. 6). Hence, GS were associated with high evaporation and relatively dry conditions in Petén Itzá. Previously, Correa-Metrio et al., (2012) provided a high-resolution record of pollen and carbonized material in the Site PI-6 record (~200 year-resolution), which demonstrated an increase in forest fires in this region during GS. This is consistent with high evaporation that is in response to dry conditions in the northern Neotropics. The latter is more apparent for GS13, GS9 and GS5, whose presence in the record is synchronous with the North Atlantic IRD deposits associated with HS5-3, respectively. The enhanced Ca/Ti+Al+Fe ratios during GS13, GS9 and GS5 in Lake Petén Itzá may be a response to dry conditions that dominated during HS. In addition, higher abundances of gypsum were found during GS13 and GS9 suggesting high evaporation in the lake. Similar increases in Ca/Ti+Al+Fe ratios and gypsum content are observed during GS8, GS7, GS5, GS4 and GS3. We did not observe an increase in gypsum content during the GS11, GS10 and GS6, which is likely due to the low sampling resolution in this interval, but in which the Ca/Ti+Al+Fe ratio suggests an increase in evaporation. Samples putatively corresponding to GS14, GS12 and GS2 cannot be identified unequivocally based on the gypsum content. This may be caused by the following reasons: First, GS14 and 12 are located in a depth interval with a relatively high uncertainty of the Petén Itzá age-depth model, which makes the identification of both GS difficult. Second, GS2 is linked to the beginning of

the LGM which, as discussed above, is characterized by high humidity in Petén Itzá. This likely suppressed the GS2 signal in the sediments.

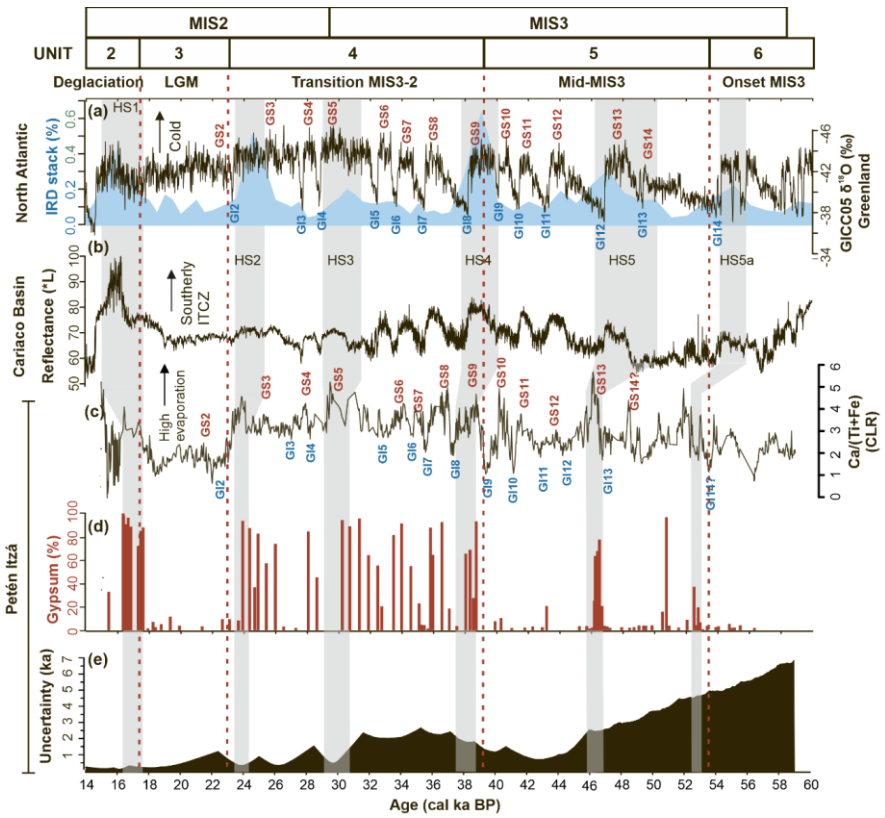

Figure 86. Temporal variation of climate proxies in the Petén Itzá PI-2 sediment record ~~data~~ compared to other paleoclimat~~ic~~ records covering the time span from ~~between~~ 60 ~~and~~ to 14 cal ka BP. a~~A~~) North Atlantic ice rafted debris (IRD) stack derived from 15 individual sediment cores ~~(presented by~~ Lisiecki and Stern, ~~(~~2016)~~. (Blue area).~~ Oxygen isotopes ($\delta^{18}O$) from the GICC05 ice core from Greenland (Svensson et al., 2008). More negative values represent colder intervals used to define Greenland Stadials (GS), more positive values represent warmer periods corresponding to ~~ice core record in Greenland (black solid line), less negative values are warmer intervals used to define~~ Greenland Interstadials (GI). b~~B~~) Reflectance L* from ~~the~~ Cariaco Basin sediments, reported by Deplazes et al.~~,~~ (2013)~~., lower~~ Higher values indicate a ~~north~~ southward migration of the Intertropical Convergence Zone (ITCZ). c~~C~~) ~~Titanium (Ti) data from the PI-2 record. D)~~ Ca/(Ti~~+Al~~+Fe) ratios~~ ratios (black line) and~~, d) gypsum content~~data (red bars) from the PI-2 record~~. e~~E~~) Uncertainty of the age-depth model. ~~across the PI-2 sequence. Numbers GI2-14 refer to GI.~~ Gray shaded areas represent HS. ~~GS recognized in the gypsum data are indicated with red labels.~~

Con formato: Espacio Antes: 12 pto, No conservar con el siguiente

Con formato: Color de fuente: Automático

Table 3. Chronology of Heinrich Stadials in the PI-2 record compared with glaciomarine records. The asterisk (*) refers to the beginning of each HS. Double asterisks (**) refer to the time of maximal IRD deposition. MCD = master composite depth.

	Depth site PI-2 (MCD) [m]	Age PI-2 [cal ka BP]	Age [cal ka BP] (Hemming, 2004) *	Age [cal ka BP] (Jullien et al., 2006, 2007)	Age [cal ka BP] (Hodell et al., 2010) **	Age [cal ka BP] (Lisiecki and Stern, 2016) **
HS1	24.77-22.28	17.7-16.3	16.8	18.3-16.0	16.0	16.0
HS2	30.13-29.63	24.3-23.7	24.0	26.2-24	24.0	24.5
HS3	35.37-34.17	31.5-29.4	31.0	31.8-30.2	-	30.5
HS4	43.99-41.40	39.2-37.5	38.0	40.2-38.2	39.6	39.0
HS5	51.40-50.80	47.0-46.2	45.0	50.0-47.9	47.5	47.0

The new age-depth model established here shows that gypsum sand layers were deposited during the cold stages HS4-1, in agreeingment with results by previous works in Lake Petén Itzá (Hodell et al., (2008), ; Mueller et al., (2010) and; Escobar et al., (2012) and with the HS chronology from variousmultiple glaciomarine records across the North Atlantic (Labeyrie et al., 1995; Hemming, 2004; Shackleton et al., 2004; Jullien et al., 2006, 2007; Hodell et al., 2010; Appendix D)). With regard to the age uncertainty, Following the discussion above regarding the tuning the Petén Itzá and Cariaco Basin sequences, the recognition of HS5 is likely found would be established between GI13 and 12 (49.3-46 cal ka BP), also corresponding to a period characterized by gypsum the deposition of gypsum. Lake Petén Itzá sediments associated with HS5-1 show Ti below average for the entire sequence, revealing high evaporation and low runoff, associated with dry conditions during their deposition.

Ages of these gypsum deposits correspond with the HS chronology presented previously for various glaciomarine records across the North Atlantic (Labeyrie et al., 1995; Hemming, 2004; Shackleton et al., 2004; Jullien et al., 2006, 2007; Hodell et al., 2010) and the compilation of several sedimentary marine records from the Atlantic, Pacific and Indian Oceans (Lisiecki and Stern, 2016; Table 3). Sediments associated with HS5-1 show Ti values below the average compared to the entire sequence (-2.2), revealing high evaporation and low runoff associated with dry conditions during their deposition. Values found in HS3 are slightly lower (-4.6) than observed in other HS, which suggests that this stage was likely characterized by driest conditions of the investigated sequence.

Similarities between records from Sites PI-6 and PI-2 confirm the overall suitability of Lake Petén Itzá sediments as hydroclimate archive. Our inferences are similar to the reconstructed record from Site PI-6, confirming that the lake response to hydroclimate change was the same among sites in the lake. Ostracod data, for example, suggest that HS3-1 were characterized by high lake-water conductivity, associated with an increase in evaporation and a reduction in runoff (Cohuo et al., 2018; Pérez et al., 2021). In addition, pollen records show the establishment of savanna vegetation, associated with dry conditions and a drop-in mean annual air temperatureMAAT of up to 6°C (Correa-Metrio et al., 2012; Hodell et al., 2012). Moreover, $\delta^{13}C$ and $\delta^{18}O$ values in ostracods indicate a lake level lowering of lake level such that Site Site PI-6 was in such shallow waters that the overlying water column did not stratify thermallywithin the oxygen-rich epilimnion (Escobar et al., 2012). This is in agreements with paleoclimate records from the Eastern

Equatorial Pacific, the Caribbean and Central Mexico (Leduc et al., 2007; Arienzo et al., 2015, 2017; Medina-Elizalde et al., 2017; Hodell et al., 2017; Caballero et al., 2019), which suggests that HS4-1 were generally dry and cold. The dry response in Lake Petén Itzá during ~~the~~ HS correlates with the ~~worldwide~~ globally recognized "Tropical Hydroclimatic Events (THEs)", ~~in~~ during which extreme regional anomalies in rainfall occurred (Bradley and Díaz, 2021~~0~~). The dominance of dry conditions in the Caribbean region during THEs was favored by meltwater input to the North Atlantic that, in turn, reduced the ~~Atlantic Meridional Oceanic Circulation~~AMOC. As a result, the mean position of the ITCZ moved approximately 1° to the south, promoting droughts not only in the northern Neotropics but also in Africa and the Arabian Peninsula (Tjallingii et al., 2008; Zarriess et al., 2011).

A key finding of our high-resolution record is confirmation of the abruptness of millennial-scale hydroclimate shifts, which enabled us to link them to AMOC shifts, rather than to gradual longer-term changes caused by orbital forcing, which underlie the short-term, abrupt climate excursions. The spatio-temporal paleoclimate changes (Fig. 7) identified from various records across the Neotropics imply that the causes of transient vs. rapid shifts in the region are more complex than mere latitudinal shifts in the ITCZ in response to AMOC. In particular, meridional inter-basin changes in the SST gradient between the Pacific and Atlantic appear to have influenced shifts in the strength and location of deep convection linked to the CLLJ that steered moisture into some parts of the Neotropics, while other areas were dry. Our results are conceptionally consistent with findings from recent climate modelling of the SE-Asian monsoon region during the late glacial, which show that regional changes in atmospheric deep convection in response to SST changes can cause strong regional hydroclimate contrasts linked to meridional shifts in low pressure centers, rather than only latitudinal shifts in the position of the ITCZ (Hällberg et al. 2022).

~~5~~6 Conclusions

We ~~U~~used~~ing~~ the sediment record from Site PI-2 in Lake Petén Itzá to ~~in Lake Petén Itzá, we~~ infer~~red~~ changes in runoff, evaporation intensity, organic matter provenance and redox conditions during MIS3-2 (59-15 cal ka BP). The onset and middle of MIS3 (59-39.2 cal ka BP) was characterized by ~~a~~ period~~s~~ of high precipitation and runoff into Lake Petén ~~variability in Lake Petén~~ Itzá. At that time, lake levels were high, the lake was highly productive and bottom water anoxia persisted. The MIS3-2 transition (39-24 cal ka BP) ~~with large changes in runoff and evaporation on millennial time scales. The end of MIS3 (39.3-29 cal ka BP), however,~~ was characterized by a gradual decline in runoff and an increase in evaporation but it was accompanied by high climate variability indicative of regional climate instability. This regime shift was accompanied by input of mixed aquatic and terrestrial organic matter and more oxygenated bottom waters, ~~perhaps~~ related to low~~er~~ ~~water~~ lake levels towards the end of MIS3. ~~near the end of MIS3.~~ MIS2 was a dry period with low runoff, ~~with the exception of the Last Glacial Maximum~~except for the LGM, during which ~~when~~ wet conditions prevailed. During the LGM, lake sediments received greater~~relatively greater~~

Con formato: Color de fuente: Automático

Con formato: Color de fuente: Automático

~~contributions~~ inputs of aquatic organic matter, and the lake hypolimnion ~~etic waters were~~was ~~-~~persistently anoxic, presumably associated with deep-water conditions.

Both GS and GI were detected in the sediment record at Site PI-2. Compared to previous studies, the record from Site PI-2 provides greater temporal resolution and demonstrates that GS 9, 8, 7 and 6 began with abrupt increases in evaporation and ended with gradual increases in humidity, whereas GS 11 and 10 showed the reverse pattern. This can be explained by the lack of moisture transported by the CLLJ during GS9-6, which made the local climate susceptible to changes in the latitudinal position of the ITCZ. The high resolution of the PI-2 record highlights the abruptness of climate shifts, which are tied to abrupt shifts in the strength of AMOC.

Comparison of our climate proxy records with other terrestrial and marine paleoclimate ~~regional~~ data from the northern Neotropics, the Caribbean, Florida, and northern Mexico indicates that variability in precipitation and in turn, runoff, ~~and consequently precipitation in the region~~ during MIS3-2, was strongly influenced by ~~the~~ latitudinal shifts in position ~~migration~~ of the ITCZ in response to changes in the strength of the AMOC. Changes in the intensity of the CLLJ and the transport of moisture by the NAM to northern Mexico also influenced fluctuations in runoff. Short-term changes in Ti and Ca/(Ti+Fe) indicate that latitudinal ITCZ variations during MIS3-2 modified runoff on short (millennial) timescales in response to AMOC shifts, whereas the CLLJ, whose strength/weakening depends on the ΔSST between the Pacific and the Caribbean, among other factors such as the extension of the NASH and the interaction with the ITZC, additionally influenced the ingress of moisture into the region on longer time scales. While our study suggests the importance of inter-basin SST differences in defining regional moisture changes via the strength of the CLLJ on longer timescales, in addition to shifts in the ITCZ, more records and additional modelling studies are required to disentangle the importance of interhemispheric changes (ITCZ) and inter-basin changes (CLLJ) on different timescales.

~~Millennial climate events such as GI14-2, GS14-2 and HS5-1 were identified in the PI-2 record and show similar responses to those reconstructed for Site PI-6. HS and GS were marked by high evaporation in Lake Petén Itzá associated with dry conditions. In particular, GS13, 9 and 5 showed dry conditions as they were contemporaneous to HS5 to 3, respectively. Moreover, GIs were associated with high runoff and low evaporation in the lake linked to the dominance of wet conditions in the region. Overall, GIs in Petén Itzá were marked by relatively wet environments, with high runoff and precipitation in sediments older than 35 kyr possibly linked to a persistent northern position of the ITCZ. The Petén Itzá sediments offer one of the few records from the northern edge of the Neotropics that has adequate resolution for the identification and future studies of millennial climate oscillations.~~

Author contribution

All of the authors listed made substantial contributions to the manuscript ~~and qualify for authorship~~. RMA, AS, LP and TB directed the research and participated in drafting the manuscript; DH, MB, JC, DA, and FA led the Petén Itzá Scientific Drilling Project. ~~that collected and described the cores and obtained the m~~Material used for radiocarbon dating that was ~~done~~ obtained by TG. ~~-~~MA, PH, DH and SK reviewed the data; MB, DH, SC, LMG, MS, JC, FA, DA, TG, ACM and FS contributed to the interpretation and discussion of the ~~reviewed the~~ manuscript ~~critically~~. ~~We acknowledge that all the authors have agreed to this submission.~~

Con formato: Color de fuente: Automático

Con formato: Color de fuente: Automático

Competing interests:

The authors declare that they have no conflict of interest.

Acknowledgments

We thank ~~all~~ our many colleagues and the institutions involved in the Petén Itzá Drilling Project. In particular, we thank Andreas Mueller, Jaime Escobar, Adrian Gilli, Florence Sylvestre, Dominik Schmidt, Esmeralda Cruz, Mark Bush, as well as Kristina Brady, Anders Noren and others ~~colleagues~~ from the National Lacustrine Core Repository (LacCore, now Continental Scientific Drilling [CSD] Facility), University of Minnesota,~~)~~ for their participation and for organizing and providing data. We especially thank Jonathan Obrist-Farner, Rik Tjallingii and Robert Brown for advising and helping during the geochemical analyses and data normalization~~helping during calibration analyses~~. We are grateful to Sophie Warken, Sarah Metcalfe and one anonymous reviewer for comments that improved the manuscript. Funding for this publication was provided by the Deutsche Forschungsgemeinschaft (DFG grants 5448462, 235297191, 252760755, 439719305, KU2685/3-1 and SCHW671/16-1) and~~,~~ Technische Universitat Braunschweig~~,~~. US National Science Foundation (ATM-0502030), Swiss National Science Foundation (grant 620-066113), the Swedish Research Council for Sustainable Development (FORMAS grant 2020-01000) and the ~~International Continental Scientific Drilling Program~~ICDP provided funding and material during the drilling campaign.

References

Amador, J.A., Magaña, V.O., and Pérez, J.B.: The low-level jet and convective activity in the Caribbean. In Proc. 24th Conf. on Hurricanes and Tropical Meteorology American Meteorological Society: Fort Lauderdale, 114–115, 2000.

Anselmetti, F. S., Ariztegui, D., Hodell, D. A., Hillesheim, M. B., Brenner, M., Gilli, A., McKenzie, J.A., and Mueller, A. D.: Late Quaternary climate-induced lake level variations in Lake Petén Itzá, Guatemala, inferred from seismic stratigraphic analysis, Palaeogeogr. Palaeoclimatol. Palaeoecol., 230 ~~(1-2)~~, 52-69, https://doi.org/10.1016/j.palaeo.2005.06.037, 2006.

Arienzo, M.M., Swart, P.K., Pourmand, A., Broad, K., Clement, A.C., Murphy, L.N., Vonhof, H.B., and Kakuk, B.: Bahamas speleothem reveals climate variability associated with Heinrich events. Earth Planet. Sci. Lett. 430, 377-386, https://doi.org/10.1016/j.epsl.2015.08.035, 2015.

Arienzo, M. M., Swart, P. K., Broad, K., Clement, A. C., Pourmand, A., and Kakuk, B.: Multi-proxy evidence of millennial climate variability from multiple Bahamian speleothems, Quat. Sci. Rev., 161, 18-29, https://doi.org/10.1016/j.quascirev.2017.02.004, 2017.

Con formato: Color de fuente: Automático
Con formato: Color de fuente: Automático
Código de campo cambiado
Código de campo cambiado
Con formato: Color de fuente: Automático
Con formato: Color de fuente: Automático
Con formato: Color de fuente: Automático
Con formato: Color de fuente: Automático
Código de campo cambiado

Bard, E., Rostek, F., Turon, J.L., and Gendreau, S.: Hydrological impact of Heinrich events in the subtropical Northeast Atlantic. Science, 289, 1321–1324, https://doi.org/10.1126/science.289.5483.1321, 2000.

Blaauw, M: Out of tune: the dangers of aligning proxy archives, Quat. Sci. Rev., 36, 38-49, https://doi.org/10.1016/j.quascirev.2010.11.012, 2012.

Blaauw, M., and Christen, J. A.: Flexible paleoclimate age-depth models using an autoregressive gamma process, Bayesian Anal., 6(3), 457-474, https://doi.org/10.1214/11-BA618, 2011.

Bloemsma, M. R.: Development of a modelling framework for core data integration using XRF scanning, Ph.D. thesis, Delft University of Technology, Netherlands, 229 pp., 2015.

Bradbury, J. P.: Sources of glacial moisture in Mesoamerica, Quat. Int., 43, 97-110, https://doi.org/10.1016/S1040-6182(97)00025-6, 1997.

Bradbury, J. P.: Limnologic history of Lago de Patzcuaro, Michoacan, Mexico for the past 48,000 years: impacts of climate and man, Palaeogeogr. Palaeoclimatol. Palaeoecol., 163(1-2), 69-95, https://doi.org/10.1016/S0031-0182(00)00146-2, 2000.

Bradley, R. S., and Diaz, H. F.: Late Quaternary abrupt climate change in the tropics and sub-tropics: The continental signal of Tropical Hydroclimatic Events (THEs), Rev. Geophys., 59 (4), https://doi.org/10.1029/2020RG000732, 2021.

Broecker, W., Bond, G., Klas, M., Clark, E., and McManus, J.: Origin of the northern Atlantic's Heinrich events, Climate Dynamics, 6(3), 265-273, https://doi.org/10.1007/BF00193540, 1992.

Boggs, S. (Ed.): Principles of sedimentology and stratigraphy, Pearson Prentice Hall, New Jersey, USA, 2006.

Boyle, J. F.: Organic geochemical methods in palaeolimnology, in: Tracking environmental change using lake sediments, edited by: Last, W., and Smol, J.P., Springer, Dordrecht, The Netherlands, 83-141, 2001.

Burns, S. J., Fleitmann, D., Matter, A., Neff, U., and Mangini, A.: Speleothem evidence from Oman for continental pluvial events during interglacial periods, Geology, 29(7), 623-626, https://doi.org/10.1130/0091-7613(2001)029%3C0623:SEFOFC%3E2.0.CO;2, 2001.

Bush, M. B., Correa-Metrio, A. Y., Hodell, D. A., Brenner, M., Anselmetti, F. S., Ariztegui, D., Mueller, A. D., Curtis, J. H., Grzesik, D. A., Burton, C., and Gilli, A.: Re-evaluation of climate change in lowland Central America during the Last Glacial Maximum using new sediment cores from Lake Petén Itzá, Guatemala, in: Past climate variability in South America and surrounding regions, edited by: Vimeux, F., Sylvestre, F., Khodri, M., Springer, Dordrecht, The Netherlands, 113-128, https://doi.org/10.1007/978-90-481-2672-9_5, 2009.

Caballero, M., and Vázquez, G.: Mixing patterns and deep chlorophyll a maxima in an eutrophic tropical lake in western Mexico, Hydrobiologia, 847(20), 4161-4176, https://doi.org/10.1007/s10750-020-04367-y, 2020.

Código de campo cambiado
Con formato: Color de fuente: Automático
Con formato: Color de fuente: Automático
Con formato: Color de fuente: Automático
Código de campo cambiado
Código de campo cambiado
Con formato: Color de fuente: Automático
Con formato: Color de fuente: Automático
Con formato: Color de fuente: Automático
Código de campo cambiado
Con formato: Color de fuente: Automático
Con formato: Color de fuente: Automático
Código de campo cambiado
Con formato: Color de fuente: Automático
Con formato: Color de fuente: Automático
Código de campo cambiado
Con formato: Color de fuente: Automático
Con formato: Color de fuente: Automático
Código de campo cambiado
Con formato: Color de fuente: Automático
Con formato: Color de fuente: Automático
Código de campo cambiado
Con formato: Color de fuente: Automático
Con formato: Color de fuente: Automático
Código de campo cambiado
Con formato: Color de fuente: Automático
Con formato: Color de fuente: Automático
Código de campo cambiado
Con formato: Color de fuente: Automático
Con formato: Color de fuente: Automático

Caballero, M., Lozano, S., Ortega, B., Urrutia, J., and Macias, J. L.: Environmental characteristics of Lake Tecocomulco, northern basin of Mexico, for the last 50,000 years, J Paleolimnol., 22~~(4)~~, 399-411, https://doi.org/10.1023/A:1008012813412, 1999.

Caballero, M., Lozano-García, S., Ortega-Guerrero, B., and Correa-Metrio, A.: Quantitative estimates of orbital and millennial scale climatic variability in central Mexico during the last~ 40,000 years, Quat. Sci. Rev., 205, 62-75, https://doi.org/10.1016/j.quascirev.2018.12.002, 2019.

Chávez-Lara, C. M., Roy, P. D., Caballero, M. M., Carreño, A. L., and Lakshumanan, C.: Lacustrine ostracodes from the Chihuahuan Desert of Mexico and inferred Late Quaternary paleoecological conditions, Rev. Mex. de Cienc. Geol., 29~~(2)~~, 422-431, http://www.scielo.org.mx/scielo.php?script=sci_arttext&pid=S1026-87742012000200010&lng=es&nrm=iso, 2012.

Clark, P. U., Marshall, S. J., Clarke, G. K., Hostetler, S. W., Licciardi, J. M., and Teller, J. T.: Freshwater forcing of abrupt climate change during the last glaciation, Science, 293~~(5528)~~, 283-287, https://doi.org/10.1126/science.1062517, 2001.

Cohuo, S., Macario-González, L., Pérez, L., and Schwalb, A.: Overview of Neotropical-Caribbean freshwater ostracode fauna (Crustacea, Ostracoda): identifying areas of endemism and assessing biogeographical affinities, Hydrobiologia, 1-17, https://doi.org/10.1007/s10750-016-2747-1, 2017.

Cohuo, S., Macario-González, L., Pérez, L., Sylvestre, F., Paillès, C., Curtis, J. H., Kuterolf, S., Wojewódka, M., Zawisza, E., Szeroczynska, K., and Schwalb, A.: Climate ultrastructure and aquatic community response to Heinrich Stadials (HS5a-HS1) in the continental northern Neotropics, Quat. Sci. Rev., 197, 75-91, https://doi.org/10.1016/j.quascirev.2018.07.015, 2018.

Cohuo, S., Macario-González, L., Wagner, S., Naumann, K., Echeverría-Galindo, P., Pérez, L., Curtis, J., Brenner, M., and Schwalb, A: Influence of late Quaternary climate on the biogeography of Neotropical aquatic species as reflected by non-marine ostracodes. Biogeosciences, 17~~(1)~~, 145-161, https://doi.org/10.5194/bg-17-145-2020, 2020.

Correa-Metrio, A., Bush, M. B., Cabrera, K. R., Sully, S., Brenner, M., Hodell, D. A., Escobar, J., and Guilderson, T.: Rapid climate change and no-analog vegetation in lowland Central America during the last 86,000 years. Quat. Sci. Rev., 38, 63-75, https://doi.org/10.1016/j.quascirev.2012.01.025, 2012.

~~Dansgaard, W., Johnsen, S. J., Clausen, H. B., Dahl-Jensen, D., Gundestrup, N. S., Hammer, C. U., Hvidberg, C.S., Steffensen, J.P. Sveinbjörnsdottir, A.E. Jozuel, J., and Bond, G.: Evidence for general instability of past climate from a 250-kyr ice-core record, Nature, 364(6434), 218-220, https://doi.org/10.1038/364218a0, 1993.~~

Davies, H.: Quaternary Palaeolimnology of a Mexican Crater Lake. Ph.D. thesis, University of Kingston, United Kingdom, 248 pp., 1995.

Davies, S., Lamb, H., and Roberts, S.: Micro-XRF Core Scanning in Palaeolimnology: Recent Developments, in: Micro-XRF Studies of Sediment Cores. Developments in Paleoenvironmental Research Vol.17, edited by: Croudace,

Código de campo cambiado
Con formato: Color de fuente: Automático
Con formato: Color de fuente: Automático
Código de campo cambiado
Con formato: Color de fuente: Automático
Con formato: Color de fuente: Automático
Con formato: Color de fuente: Automático
Código de campo cambiado
Con formato: Color de fuente: Automático
Código de campo cambiado
Con formato: Color de fuente: Automático
Con formato: Color de fuente: Automático
Código de campo cambiado
Con formato: Color de fuente: Automático
Con formato: Color de fuente: Automático
Código de campo cambiado
Con formato: Color de fuente: Automático
Con formato: Color de fuente: Automático
Código de campo cambiado
Con formato: Color de fuente: Automático
Con formato: Color de fuente: Automático
Código de campo cambiado
Con formato: Color de fuente: Automático
Con formato: Color de fuente: Automático
Código de campo cambiado
Con formato: Color de fuente: Automático
Con formato: Color de fuente: Automático

I., and Rothwell, R., Springer, Dordrecht. The Netherlands, 189-226, https://doi.org/10.1007/978-94-017-9849-5_7, 2015.

Dean, W. E.: The carbon cycle and biogeochemical dynamics in lake sediments, J Paleolimnol, 21(4), 375-393, https://doi.org/10.1023/A:1008066118210, 1999.

Deplazes, G., Lückge, A., Peterson, L. C., Timmermann, A., Hamann, Y., Hughen, K. A., Röhl, U., Laj, C., Cane, M.A., Sigman D.M. and Haug, G. H.: Links between tropical rainfall and North Atlantic climate during the last glacial period. Nat. Geosci., 6(3), 213-217, https://doi.org/10.1038/ngeo1712, 2013.

Díaz, K.A., Pérez, L., Correa-Metrio, A., Franco-Gaviria, J.F., Echeverría, P., Curtis, J., and Brenner, M.: Holocene environmental history of tropical, mid-altitude Lake Ocotalito, México, inferred from ostracodes and non-biological indicators, The Holocene, 27(9), 1308-1317, https://doi.org/10.1177%2F0959683616687384, 2017.

Donders, T. H., de Boer, H. J., Finsinger, W., Grimm, E. C., Dekker, S. C., Reichart, G. J., and Wagner-Cremer, F.: Impact of the Atlantic Warm Pool on precipitation and temperature in Florida during North Atlantic cold spells, Climate Dynamics, 36(1-2), 109-118, https://doi.org/10.1007/s00382-009-0702-9, 2011.

Dunlea, A. G., Murray, R. W., Tada, R., Alvarez-Zarikian, C. A., Anderson, C. H., Gilli, A., Giosan, L., Gorgas, T., Hennekam, R., Irino T., Murayama, M., Peterson, L., Reichart, G.J. Seki, A., Zheng, H., and Ziegler, M.: Intercomparison of XRF core scanning results from seven labs and approaches to practical calibration, Geochemistry, Geophys. Geosystems, 21(9), https://doi.org/10.1029/2020GC009248, 2020.

Echeverría Galindo, P. G., Pérez, L., Correa-Metrio, A., Avendaño, C. E., Moguel, B., Brenner, M., Cohuo, S., Macario, L., Caballero, M., and Schwalb, A.: Tropical freshwater ostracodes as environmental indicators across an altitude gradient in Guatemala and Mexico, Rev. Biol. Trop., 67(4), 1037-1058. https://doi.org/10.15517/RBT.V67I4.33278, 2019.

Engleman, E. E., Jackson, L. L., and Norton, D. R.: Determination of carbonate carbon in geological materials by coulometric titration, Chem. Geol., 53(1-2), 125-128, 1985

Engstrom, D. R., and Wright Jr, H. E.: Chemical stratigraphy of lake sediments as a record of environmental change, in: Lake sediments and environmental history: studies in palaeolimnology and palaeoecology in honour of Winifred Tutin, edited by: Haworth, E.Y. and Lund, J.W.G., Leicester University Press, United Kingdom, 1984.

Escobar, J., Hodell, D. A., Brenner, M., Curtis, J. H., Gilli, A., Mueller, A. D., Anselmetti F.S. Ariztegui D., Grzesik D.A., Pérez, L., Schwalb A., and Guilderson, T. P.: A~ 43-ka record of paleoenvironmental change in the Central American lowlands inferred from stable isotopes of lacustrine ostracods, Quat. Sci. Rev., 37, 92-104, https://doi.org/10.1016/j.quascirev.2012.01.020, 2012.

Friedrich, J., Janssen, F., Aleynik, D., Bange, H. W., Boltacheva, N., Çagatay, M. N., Dale, A.W., et al.: Investigating hypoxia in aquatic environments: diverse approaches to addressing a complex phenomenon, Biogeosciences, 11(4), 1215-1259, https://doi.org/10.5194/bg-11-1215-2014, 2014.

Código de campo cambiado
Con formato: Color de fuente: Automático
Con formato: Color de fuente: Automático

Gale, E., Pattiaratchi, C., and Ranasinghe, R.: Vertical mixing processes in intermittently closed and open lakes and lagoons, and the dissolved oxygen response, Estuar. Coast. Shelf Sci., 69(1-2), 205-216, https://doi.org/10.1016/j.ecss.2006.04.013, 2006

Gibson, K. A., and Peterson, L. C.: A 0.6 million year record of millennial-scale climate variability in the tropics. Geophys. Res. Lett., 41(3), 969-975, https://doi.org/10.1002/2013GL058846, 2014.

Grauel, A.-L., Hodell, D.A., and Bernasconi, S.M.: Quantitative estimates of tropical temperature change in lowland Central America during the last 42 ka, Earth Planet. Sci. Lett., 438, 37–46, https://doi.org/10.1016/j.epsl.2016.01.001, 2016.

Grimm, E. C., Watts, W. A., Jacobson Jr, G. L., Hansen, B. C., Almquist, H. R., and Dieffenbacher-Krall, A. C.: Evidence for warm wet Heinrich events in Florida, Quat. Sci. Rev., 25(17-18), 2197-2211, https://doi.org/10.1016/j.quascirev.2006.04.008, 2006.

~~Grauel, A.-L., Hodell, D.A., and Bernasconi, S.M.: Quantitative estimates of tropical temperature change in lowland Central America during the last 42 ka, Earth Planet. Sci. Lett., 438, 37–46, https://doi.org/10.1016/j.epsl.2016.01.001, 2016.~~

Groot, M. H. M., Lourens, L. J., Hooghiemstra, H., Vriend, M., Berrio, J. C., Tuenter, E., Van der Plicht, J., Van Geel, B., Ziegler, M., Weber, S. L., Betancourt, A., et al.: Ultra-high resolution pollen record from the northern Andes reveals rapid shifts in montane climates within the last two glacial cycles, Clim. Past, 7(1), 299-316, https://doi.org/10.5194/cp-7-299-2011, 2011.

Groot, M. H., Hooghiemstra, H., Berrio, J. C., and Giraldo, C.: North Andean environmental and climatic change at orbital to submillennial time-scales: vegetation, water levels and sedimentary regimes from Lake Fúquene 130–27 ka. Rev. Palaeobot. Palynol., 197, 186-204, https://doi.org/10.1016/j.revpalbo.2013.04.005, 2013.

Grousset, F. E., Pujol, C., Labeyrie, L., Auffret, G., and Boelaert, A.: Were the North Atlantic Heinrich events triggered by the behavior of the European ice sheets?, Geol. J, 28, 123-126, https://doi.org/10.1130/0091-7613(2000)28<123:WTNAHE>2.0.CO;2, 2000.

Hällberg, P.L., Schenk, F., Yamoah, K.A., Kuang, X., and Smittenberg, R.H.: Seasonal aridity in the Indo-Pacific Warm Pool during the Late Glacial driven by El Niño-like conditions, Clim. Past, 18, 1655-1674, https://doi.org/10.5194/cp-18-1655-2022, 2022.

Heinrich, H.: Origin and consequences of cyclic ice rafting in the Northeast Atlantic Ocean during the past 130,000 years, Quat. Res., 29, 143–152, https://doi.org/10.1016/0033-5894(88)90057-9, 1988.

Hemming, S. R.: Heinrich events: Massive late Pleistocene detritus layers of the North Atlantic and their global climate imprint, Rev. Geophys., 42(1), https://doi.org/10.1029/2003RG000128, 2004.

Con formato: Color de fuente: Automático
Código de campo cambiado
Con formato: Color de fuente: Automático
Código de campo cambiado
Con formato: Color de fuente: Automático
Código de campo cambiado
Con formato: Color de fuente: Automático
Con formato: Color de fuente: Automático
Código de campo cambiado
Con formato: Color de fuente: Automático
Con formato: Color de fuente: Automático
Código de campo cambiado
Con formato: Color de fuente: Automático
Con formato: Color de fuente: Automático
Con formato: Color de fuente: Automático
Con formato: Color de fuente: Automático
Código de campo cambiado
Código de campo cambiado
Con formato: Color de fuente: Automático
Con formato: Color de fuente: Automático
Código de campo cambiado
Con formato: Color de fuente: Automático
Con formato: Inglés (Estados Unidos)
Con formato: Fuente: (Predeterminada) Times New Roman, 10 pto, Color de fuente: Automático
Código de campo cambiado
Con formato: Color de fuente: Automático
Con formato: Color de fuente: Automático
Código de campo cambiado
Con formato: Color de fuente: Automático
Con formato: Color de fuente: Automático

Hodell, D., Anselmetti, F., Brenner, M., and Ariztegui, D.: The Lake Petén Itzá Scientific Drilling Project, Sci. Drill., 3, 25-29, https://doi.org/10.2204/iodp.sd.3.02.2006, 2006.

Hodell, D. A., Anselmetti, F. S., Ariztegui, D., Brenner, M., Curtis, J. H., Gilli, A., Grzesik, D.A., Guilderson, T.J., Mueller A. D., Bush, M.B., Correa-Metrio, A., Escobar, J., and Kutterolf, S.: An 85-ka record of climate change in lowland Central America. Quat. Sci. Rev., 27~~(11-12)~~, 1152-1165, https://doi.org/10.1016/j.quascirev.2008.02.008, 2008.

Hodell, D. A., Evans, H. F., Channell, J. E., and Curtis, J. H.: Phase relationships of North Atlantic ice-rafted debris and surface-deep climate proxies during the last glacial period, Quat. Sci. Rev., 29~~(27-28)~~, 3875-3886., https://doi.org/10.1016/j.quascirev.2010.09.006, 2010.

Hodell, D.A., Turchyn, A.V., Wiseman, C.J., Escobar, J., Curtis, J.H., Brenner, M., Gilli, A., Mueller, A.D., Anselmetti, F., Ariztegui, D., and Brown, E.T.: Late Glacial temperature and precipitation changes in the lowland Neotropics by tandem measurements of $\delta^{18}O$ in biogenic carbonate and gypsum hydration water, Geochim. Cosmochim. Acta 77, 352–368, https://doi.org/10.1016/j.gca.2011.11.026, 2012.

Hodell, D. A., Nicholl, J. A., Bontognali, T. R., Danino, S., Dorador, J., Dowdeswell, J. A., Einsle, J., Kuhlmann H., Martrat, B., Mleneck-Vautravers, M.J., Rodríguez-Tovar, F.J., and Röhl, U.: Anatomy of Heinrich Layer 1 and its role in the last deglaciation, Paleoceanography, 32~~(3)~~, 284-303, https://doi.org/10.1002/2016PA003028, 2017

Hu, H., and Dominguez, F.: Evaluation of oceanic and terrestrial sources of moisture for the North American monsoon using numerical models and precipitation stable isotopes. J Hydrometeorol, 16, 19-35, https://doi.org/10.1175/JHM-D-14-0073.1, 2015.

Instituto Geográfico Nacional – IGN (1970) Carta Geológica de la Republica de Guatemala. Esc: 1:500,000.

Instituto Nacional de Sismología, Vulcanología, Meteorología e Hidrología - INSIVUMEH (2021) Información meteorológica. Access by: https:// tps://gae.insivumeh.gob.gt/publico

Jaeschke, A., Rühlemann, C., Arz, H., Heil, G., and Lohmann, G.: Coupling of millennial-scale changes in sea surface temperature and precipitation off northeastern Brazil with high-latitude climate shifts during the last glacial period. Paleoceanogr Paleoclimatol, 22, https://doi.org/10.1029/2006PA001391, 2007.

Johnsen, S., Clausen, H., Dansgaard, W. et al.: Irregular glacial interstadials recorded in a new Greenland ice core. Nature, 359, 311–313, https://doi.org/10.1038/359311a0, 1992.

Jullien, E., Grousset, F. E., Hemming, S. R., Peck, V. L., Hall, I. R., Jeantet, C., and Billy, I.: Contrasting conditions preceding MIS3 and MIS2 Heinrich events, Glob Planet Change, 54~~(3-4)~~, 225-238, https://doi.org/10.1016/j.gloplacha.2006.06.021, 2006.

Código de campo cambiado
Con formato: Color de fuente: Automático
Con formato: Color de fuente: Automático
Código de campo cambiado
Con formato: Color de fuente: Automático
Con formato: Color de fuente: Automático
Con formato: Color de fuente: Automático
Con formato: Color de fuente: Automático
Código de campo cambiado
Código de campo cambiado
Con formato: Color de fuente: Automático
Con formato: Color de fuente: Automático
Con formato: Color de fuente: Automático
Código de campo cambiado
Con formato: Color de fuente: Automático
Con formato: Color de fuente: Automático
Código de campo cambiado
Con formato: Color de fuente: Automático
Código de campo cambiado
Con formato: Color de fuente: Automático
Código de campo cambiado
Con formato: Color de fuente: Automático
Código de campo cambiado
Con formato: Color de fuente: Automático
Con formato: Color de fuente: Automático

Jullien, E., Grousset, F., Malaizé, B., Duprat, J., Sanchez-Goni, M. F., Eynaud, F., Charlier, K., Schneider, R., Bory, A., Bout, B., and Flores, J. A.: Low-latitude "dusty events" vs. high-latitude "icy Heinrich events, Quat. Res., 68~~(3)~~, 379-386, https://doi.org/10.1016/j.yqres.2007.07.007, 2007.

Kitoh, A. and Murakami, S.: Tropical Pacific climate at the mid-Holocene and the Last Glacial Maximum simulated by a coupled ocean-atmosphere general circulation model. Paleoceanography, 17, 19-1, https://doi.org/10.1029/2001PA000724, 2002.

Kucera, M., Weinelt, M., Kiefer, T., Pflaumann, U., Hayes, A., Weinelt, M., et al.: Reconstruction of sea-surface temperatures from assemblages of planktonic foraminifera: multi-technique approach based on geographically constrained calibration data sets and its application to glacial Atlantic and Pacific Oceans. Quat Sci Rev, 24, 951-998, https://doi.org/10.1016/j.quascirev.2004.07.014, 2005.

~~Kylander, M. E., Ampel, L., Wohlfarth, B., and Veres, D.: High-resolution X-ray fluorescence core scanning analysis of Les Echets (France) sedimentary sequence: new insights from chemical proxies. J Quat Sci, 26(1), 109-117, https://doi.org/10.1002/jqs.1438, 2011.~~

Kutterolf, S., Schindlbeck, J. C., Anselmetti, F. S., Ariztegui, D., Brenner, M., Curtis, J., Schmid, D., Hodell, D.A., Mueller, A, Pérez, L., Pérez, W., Schwalb, A., Frische, M., and Wang, K.L.: A 400-ka tephrochronological framework for Central America from Lake Petén Itzá (Guatemala) sediments, Quat. Sci. Rev., 150, 200-220, https://doi.org/10.1016/j.quascirev.2016.08.023, 2016.

Labeyrie, L., Vidal, L., Cortijo, E., Paterne, M., Arnold, M., Duplessy, J.C., Vautravers, M.L., Labracherie, M., Duprat, J., Turon, J.L., Grousset, F.E., and van Weering, T.: Surface and deep hydrology of the northern Atlantic Ocean during the past 150,000 years, Philosophical Transactions of the Royal Society of London, 348, 255–264, https://doi.org/10.1098/rstb.1995.0067, 1995.

Lachniet, M.S., Johnson, L., Asmerom, Y., Burns, S J., Polyak, V., Patterson, W. P., and Azouz, A.: Late Quaternary moisture export across Central America and to Greenland: evidence for tropical rainfall variability from Costa Rican stalagmites. Quat Sci Rev, 28, 3348-3360, https://doi.org/10.1016/j.quascirev.2009.09.018, 2009.

Lachniet, M.S., Asmerom, Y., Bernal, J.P., Polyak, V.J., and Vazquez-Selem, L.: Orbital pacing and ocean circulation-induced collapses of the Mesoamerican monsoon over the past 22,000 yr. Proceedings of the National Academy of Sciences, 110, 9255-9260. https://doi.org/10.1073/pnas.1222804110, 2013.

Lachniet, M. S., Denniston, R. F., Asmerom, Y., and Polyak, V. J.: Orbital control of western North America atmospheric circulation and climate over two glacial cycles. Nat. Commun., 5~~(1)~~, 1-8., https://doi.org/10.1038/ncomms4805, 2014.

Last, W. M.: Mineralogical analysis of lake sediments, in: Tracking environmental change using lake sediments, edited by: Last, W., and Smol, J.P., Springer, Dordrecht, The Netherlands, 143-187, 2001.

Con formato: Color de fuente: Automático
Con formato: Color de fuente: Automático
Código de campo cambiado
Código de campo cambiado
Con formato: Color de fuente: Automático
Código de campo cambiado
Con formato: Color de fuente: Automático
Código de campo cambiado
Con formato: Color de fuente: Automático
Con formato: Color de fuente: Automático
Código de campo cambiado
Con formato: Color de fuente: Automático
Con formato: Color de fuente: Automático
Código de campo cambiado
Con formato: Color de fuente: Automático
Con formato: Color de fuente: Automático
Código de campo cambiado
Con formato: Color de fuente: Automático
Código de campo cambiado
Con formato: Color de fuente: Automático
Con formato: Color de fuente: Automático

Leduc, G., Vidal, L., Tachikawa, K., Rostek, F., Sonzogni, C., Beaufort, L., and Bard, E.: Moisture transport across Central America as a positive feedback on abrupt climatic changes, Nature, 445~~(7130)~~, 908-911, https://doi.org/10.1038/nature05578, 2007.

Lisiecki, L. E., and Raymo, M. E.: A Pliocene-Pleistocene stack of 57 globally distributed benthic $\delta^{18}O$ records, Paleoceanography, 20~~(1)~~, https://doi.org/10.1029/2004PA001071, 2005.

Lisiecki, L. E., and Stern, J. V.: Regional and global benthic $\delta^{18}O$ stacks for the last glacial cycle, Paleoceanogr Paleoclimatol, 31~~(10)~~, 1368-1394, https://doi.org/10.1002/2016PA003002, 2016.

Lozano-García, S., Ortega, B., Roy, P. D., Beramendi-Orosco, L., and Caballero, M.: Climatic variability in the northern sector of the American tropics since the latest MIS 3, Quat Res., 84~~(2)~~, 262-271, https://doi.org/10.1016/j.yqres.2015.07.002, 2015.

Lozano-García, S., Torres-Rodríguez, E., Figueroa-Rangel, B., Caballero, M., Sosa-Nájera, S., Ortega-Guerrero, B., and Acosta-Noriega, C.: Vegetation history of a Mexican Neotropical basin from the late MIS 6 to early MIS 3: The pollen record of Lake Chalco. Quat Sci Rev, 297, 107830, https://doi.org/10.1016/j.quascirev.2022.107830, 2022.

Macario-González, L., Cohuo, S., Hoelzmann, P., Pérez, L., Elías-Gutiérrez, M., Caballero, M., and Schwalb, A.: Geodiversity influences limnological conditions and freshwater ostracode species distributions across broad spatial scales in the northern Neotropics, Biogeosciences, 19, 5167-5185, https://doi.org/10.5194/bg-19-5167-2022, 2022.~~Marshall, M. H., Lamb, H. F., Huws, D., Davies, S. J., Bates, R., Bloemendal, J., Boyle, J., Leng, M.J., Umer, M. and Bryant, C.: Late Pleistocene and Holocene drought events at Lake Tana, the source of the Blue Nile, Glob Planet Change, 78(3-4), 147-161, https://doi.org/10.1016/j.gloplacha.2011.06.004, 2011.~~

Martínez-Abarca, R., Lozano-García, S., Ortega-Guerrero, B., and Caballero-Miranda, M.: Incendios y actividad volcánica: historia de fuego en la cuenca de México en el Pleistoceno tardío con base en registros de material carbonizado en el lago de Chalco, Rev. Mex. de Cienc. Geol., 36~~(2)~~, 259-269, https://www.redalyc.org/articulo.oa?id=57265251009, 2019.

Martínez-Abarca, R., Ortega-Guerrero, B., Lozano-García, S., Caballero, M., Valero-Garcés, B., McGee, D., Brown, E.T., Stockhecke, M., and Hodgetts, A. G.: Sedimentary stratigraphy of Lake Chalco (Central Mexico) during its formative stages, Int J Earth Sci., 110~~(7)~~, 2519-2539, https://doi.org/10.1007/s00531-020-01964-z, 2021a

Martínez-Abarca, L. R., Lozano-García, S., Ortega-Guerrero, B., Chávez-Lara, C. M., Torres-Rodríguez, E., Caballero, M., Brown, E.T, Sosa-Najera, S., Acosta-Noriega, C., and Sandoval-Ibarra, V.: Environmental changes during MIS6-3 in the Basin of Mexico: A record of fire, lake productivity history and vegetation, J South Am Earth Sci., 109, 103231, https://doi.org/10.1016/j.jsames.2021.103231, 2021b

Código de campo cambiado
Con formato: Color de fuente: Automático
Con formato: Color de fuente: Automático
Código de campo cambiado
Con formato: Color de fuente: Automático
Con formato: Color de fuente: Automático
Con formato: Color de fuente: Automático
Con formato: Color de fuente: Automático
Código de campo cambiado
Código de campo cambiado
Con formato: Color de fuente: Automático
Con formato: Color de fuente: Automático
Código de campo cambiado
Con formato: Color de fuente: Automático
Con formato: Color de fuente: Automático
Código de campo cambiado
Con formato: Color de fuente: Automático
Con formato: Color de fuente: Automático
Código de campo cambiado
Con formato: Color de fuente: Automático
Con formato: Color de fuente: Automático
Código de campo cambiado
Con formato: Color de fuente: Automático
Con formato: Color de fuente: Automático
Código de campo cambiado
Con formato: Color de fuente: Automático
Con formato: Color de fuente: Automático

Martínez-Abarca, R., Bücker, M., Hoppenbrock, J., Flores-Orozco, A., Pita de la Paz, C., Fröhlich, K., Buckel, J., Lauke, T., Moguel, B., Bonilla, M., Rubio-Sandoval, K., Echeverría-Galindo, P., Landois, S., García, M., Caballero, M., Rodríguez, S., Morales, W., Escolero, O., Correa-Metrio, A., Wojewódka-Przybył, M., Schwarz, A., Krahn, K., Schwalb, A., and Pérez, L.: Evidence of large water-level variations found in deltaic sediments of a tropical deep lake in the karst mountains of the Lacandon forest, Mexico. J Paleolimnol, 1-23, https://doi.org/10.1007/s10933-022-00264-7, 2022.

Mason, B., and Moore, C. B. (Eds.): Principles of geochemistry (4th Edition), John Wiley & Sons, New York, USA, 1982.

Mays, J. L., Brenner, M., Curtis, J. H., Curtis, K. V., Hodell, D. A., Correa-Metrio, A., Escobar, J., Dutton, A.L., Zimmerman A. R., and Guilderson, T. P.: Stable carbon isotopes (δ^{13}C) of total organic carbon and long-chain n-alkanes as proxies for climate and environmental change in a sediment core from Lake Petén-Itzá, Guatemala, J Paleolimnol, 57(4), 307-319, https://doi.org/10.1007/s10933-017-9949-z, 2017

McManus, J., Francois, R., Gherardi, J.M., Keigwin, L.D., and Brown-Leger, S.: Collapse and rapid resumption of Atlantic meridional circulation linked to deglacial climate changes, Nature, 428, 834–837, https://doi.org/10.1038/nature02494, 2004.

Medina-Elizalde, M., Burns, S. J., Polanco-Martinez, J., Lases-Hernández, F., Bradley, R., Wang, H. C., and Shen, C. C.: Synchronous precipitation reduction in the American Tropics associated with Heinrich 2, Sci. Rep., 7(1), 1-12, https://doi.org/10.1038/s41598-017-11742-8, 2017

Megard, R. O.: Environment of deposition of CaCO3 in Elk lake, Minnesota, in: Elk Lake, Minnesota: Evidence for rapid climate change in the north-central United States, edited by: Bradbury, J.P., and Dean, E., U.S. Geological Survey, Colorado, USA, 97-115, 1993.

Metcalfe, S. E., Barron, J. A., and Davies, S. J.: The Holocene history of the North American Monsoon:'known knowns' and 'known unknowns' in understanding its spatial and temporal complexity. Quat Sci Rev, 120, 1-27, https://doi.org/10.1016/j.quascirev.2015.04.004, 2015.

~~Mestas-Nunez, A.M., Enfield, D.B., and Zhang, C.: Water vapor fluxes over the Intra-Americas Sea: seasonal and interannual variability and associations with rainfall, J. Clim., 20 (9), 1910–1922, https://doi.org/10.1175/JCLI4096.1, 2007.~~

Meyers, P. A.: Applications of organic geochemistry to paleolimnological reconstructions: a summary of examples from the Laurentian Great Lakes, Org. Geochem., 34(2), 261-289, https://doi.org/10.1016/S0146-6380(02)00168-7, 2003.

Con formato: Español (México)
Con formato: Español (México)
Con formato: Español (México)
Código de campo cambiado
Con formato: Color de fuente: Automático
Con formato: Inglés (Estados Unidos)
Con formato: Color de fuente: Automático
Con formato: Color de fuente: Automático
Código de campo cambiado
Código de campo cambiado
Con formato: Color de fuente: Automático
Con formato: Color de fuente: Automático
Código de campo cambiado
Con formato: Color de fuente: Automático
Con formato: Color de fuente: Automático
Código de campo cambiado
Con formato: Color de fuente: Automático
Código de campo cambiado
Con formato: Color de fuente: Automático
Con formato: Color de fuente: Automático
Código de campo cambiado
Con formato: Color de fuente: Automático
Con formato: Color de fuente: Automático

Meyers, P. A., and Ishiwatari, R.: Organic matter accumulation records in lake sediments, in: Physics and chemistry of lakes, edited by: Lerman, A., Imboden, D.M. and Ga, J.R., Springer, Berlin, Germany, 279-328, 1995.

Moernaut, J., Van Daele, M., Strasser, M., Clare, M. A., Heirman, K., Viel, M., Cardenas, J., Kilian, R., Ladron de Guevara, B., Pino, M., Urrutia, R., and De Batist, M.: Lacustrine turbidites produced by surficial slope sediment remobilization: a mechanism for continuous and sensitive turbidite paleoseismic records, Mar. Geol., 384, 159-176, https://doi.org/10.1016/j.margeo.2015.10.009, 2017.

Mueller, A. D.: Late Quaternary Environmental Change in the Lowland Neotropics: The Petén Itzá Scientific Drilling Project, Guatemala, Ph.D. thesis, ETH Zurich, Switzerland, 129 pp., 2009.

Mueller, A. D., Anselmetti, F. S., Ariztegui, D., Brenner, M., Hodell, D. A., Curtis, J. H., Escobar, J., Guilli, A., Grzesik D.A., Guilderson, T.P., Kutterolf, S., and Plötze, M.: Late Quaternary palaeoenvironment of northern Guatemala: evidence from deep drill cores and seismic stratigraphy of Lake Petén Itzá, Sedimentology, 57~~(5)~~, 1220-1245, https://doi.org/10.1111/j.1365-3091.2009.01144.x, 2010.

Mulder, T., Gillet, H., Hanquiez, V., Reijmer, J. J. G., Droxler, A. W., Recouvreur, A., Fabregas, N., Cavaihes, T., Fauquembergue, K., Blank, D.G. et al.: Into the deep: A coarse-grained carbonate turbidite valley and canyon in ultra-deep carbonate setting, Mar. Geol., 407, 316-333, https://doi.org/10.1016/j.margeo.2018.11.003, 2019

Naeher, S., Gilli, A., North, R. P., Hamann, Y., and Schubert, C. J.: Tracing bottom water oxygenation with sedimentary Mn/Fe ratios in Lake Zurich, Switzerland, Chem. Geol., 352, 125-133, https://doi.org/10.1016/j.chemgeo.2013.06.006, 2013.

Ortega-Guerrero, B., Avendaño, D., Caballero, M., Lozano-García, S., Brown, E. T., Rodríguez, A., García, B., Barceinas, H., Soler, M.A., and Albarrán, A.: Climatic control on magnetic mineralogy during the late MIS 6-Early MIS 3 in Lake Chalco, central Mexico, Quat Sci Rev., 230, 106163, https://doi.org/10.1016/j.quascirev.2020.106163, 2020.

Otto-Bliesner, B. L., Schneider, R., Brady, E. C., Kucera, M., Abe-Ouchi, A., Bard, E., et al.: A comparison of PMIP2 model simulations and the MARGO proxy reconstruction for tropical sea surface temperatures at last glacial maximum. Clim. Dyn., 32, 799-815, https://doi.org/10.1007/s00382-008-0509-0, 2009.

Paillès, C., Sylvestre, F., Escobar, J., Tonetto, A., Rustig, S., and Mazur, J. C.: Cyclotella petenensis and Cyclotella cassandrae, two new fossil diatoms from Pleistocene sediments of Lake Petén-Itzá, Guatemala, Central America, Phytotaxa, 351~~(4)~~, 247-263, https://doi.org/10.11646/phytotaxa.351.4.1, 2018.

Pérez, L., Frenzel, P., Brenner, M., Escobar, J., Hoelzmann, P., Scharf, B., and Schwalb, A.: Late Quaternary (24–10 ka BP) environmental history of the Neotropical lowlands inferred from ostracodes in sediments of Lago Petén Itzá, Guatemala, J Paleolimnol, 46~~(1)~~, 59, https://doi.org/10.1007/s10933-011-9514-0, 2011.

Código de campo cambiado
Con formato: Color de fuente: Automático
Con formato: Color de fuente: Automático
Código de campo cambiado
Con formato: Color de fuente: Automático
Con formato: Color de fuente: Automático
Con formato: Color de fuente: Automático
Con formato: Color de fuente: Automático
Código de campo cambiado
Código de campo cambiado
Con formato: Color de fuente: Automático
Con formato: Color de fuente: Automático
Código de campo cambiado
Con formato: Color de fuente: Automático
Con formato: Color de fuente: Automático
Código de campo cambiado
Con formato: Color de fuente: Automático
Código de campo cambiado
Con formato: Color de fuente: Automático
Con formato: Color de fuente: Automático
Código de campo cambiado
Con formato: Color de fuente: Automático
Con formato: Color de fuente: Automático

Pérez, L., Curtis, J., Brenner, M., Hodell, D., Escobar, J., Lozano, S., and Schwalb, A.: Stable isotope values ($\delta^{18}O$ & $\delta^{13}C$) of multiple ostracode species in a large Neotropical lake as indicators of past changes in hydrology, Quat Sci Rev. 66(0), 96-111, https://doi.org/10.1016/j.quascirev.2012.10.044, 2013.

Pérez, L., Correa-Metrio, A., Cohuo, S., González, L. M., Echeverria-Galindo, P., Brenner, M., Curtis, J., Kutterolf, S., Stockhecke, M., Schenk, F., Bauersachs, T., and Schwalb, A.: Ecological turnover in neotropical freshwater and terrestrial communities during episodes of abrupt climate change, Quat Res., 101, 26-36, https://doi.org/10.1017/qua.2020.124, 2021.

Peterson, L. C., Haug, G. H., Hughen, K. A., and Röhl, U.: Rapid changes in the hydrologic cycle of the tropical Atlantic during the last glacial, Science, 290 (5498), 1947-1951, https://doi.org/10.1126/science.290.5498.1947, 2000.

R Core Team (2018). R: a language and environment for statistical computing. R Foundation for Statistical Computing, Vienna. https://www.R-project.org

Ramírez-Barahona, S., and Eguiarte, L. E.: The role of glacial cycles in promoting genetic diversity in the Neotropics: the case of cloud forests during the Last Glacial Maximum, Ecol. Evol., 3(3), 725-738, https://doi.org/10.1002/ece3.483, 2013.

Reimer, P. J., Austin, W. E., Bard, E., Bayliss, A., Blackwell, P. G., Ramsey, C. B., et al.: The IntCal20 Northern Hemisphere radiocarbon age calibration curve (0–55 cal kBP), Radiocarbon, 62(4), 725-757, https://doi.org/10.1017/RDC.2020.41, 2020.

Rincón-Martínez, D., Lamy, F., Contreras, S., Leduc, G., Bard, E., Saukel, C., Blanz, T., Mackensen, A., and Tiedemann, R.: More humid interglacials in Ecuador during the past 500 kyr linked to latitudinal shifts of the equatorial front and the Intertropical Convergence Zone in the eastern tropical Pacific, Paleoceanography, 25(2), https://doi.org/10.1029/2009PA001868, 2010.

Roy, P. D., Quiroz-Jiménez, J. D., Pérez-Cruz, L. L., Lozano-García, S., Metcalfe, S. E., Lozano-Santacruz, R., López-Balbiaux, N., Sánchez-Zavala J.L., and Romero, F. M.: Late Quaternary paleohydrological conditions in the drylands of northern Mexico: a summer precipitation proxy record of the last 80 cal ka BP, Quat Sci Rev., 78, 342-354, https://doi.org/10.1016/j.quascirev.2012.11.020, 2013.

Royer, A., Malaizé, B., Lécuyer, C., Queffelec, A., Charlier, K., Caley, T., and Lenoble, A.: A high-resolution temporal record of environmental changes in the Eastern Caribbean (Guadeloupe) from 40 to 10 ka BP, Quat Sci Rev., 155, 198-212, https://doi.org/10.1016/j.quascirev.2016.11.010, 2017.

Schmidt, M.W., Vautravers, M.J., and Spero, H.J.: Western Caribbean sea surface temperatures during the late Quaternary. Geochem. Geophys. Geosystems., 7, https://doi.org/10.1029/2005GC000957, 2006.

Código de campo cambiado
Con formato: Color de fuente: Automático
Con formato: Color de fuente: Automático
Código de campo cambiado
Con formato: Color de fuente: Automático
Con formato: Color de fuente: Automático
Con formato: Color de fuente: Automático
Con formato: Color de fuente: Automático
Código de campo cambiado
Código de campo cambiado
Con formato: Color de fuente: Automático
Con formato: Color de fuente: Automático
Código de campo cambiado
Con formato: Color de fuente: Automático
Con formato: Color de fuente: Automático
Código de campo cambiado
Con formato: Color de fuente: Automático
Con formato: Color de fuente: Automático
Código de campo cambiado
Con formato: Color de fuente: Automático
Con formato: Color de fuente: Automático
Código de campo cambiado
Con formato: Color de fuente: Automático
Con formato: Color de fuente: Automático
Código de campo cambiado
Con formato: Color de fuente: Automático
Con formato: Color de fuente: Automático
Código de campo cambiado
Con formato: Color de fuente: Automático

~~Shackleton, N.J., Fairbanks, R.G., Chiu, T. C., and Parrenin, F.: Absolute calibration of the Greenland time scale: implications for Antarctic time scales and for $D^{14}C$, Quaternary Sci. Rev., 23, 1513-1522, https://doi.org/10.1016/j.quascirev.2004.03.006, 2004.~~

Simmons, C. S., Tarano, J. M. und Pinto, J. H. (Eds.): Clasificacion de reconocimiento de los suelos de la Republica de Guatemala. Ministerio de Agricultura, Guatemala City, Guatemala, 1959.

Spence, J.M., Taylor, M.A., and Chen, A.A.: The effect of concurrent seasurface temperature anomalies in the tropical Pacific and Atlantic on Caribbean rainfall. Int J Climatol., 24, 1531–1541, https://doi.org/10.1002/joc.1068, 2004

Svensson, A., Andersen, K. K., Bigler, M., Clausen, H. B., Dahl-Jensen, D., Davies, S. M., Johnsen, S.J., Muscheler, R., Parrenin, F., Rasmussen, S.O., Röthlisberger, R., Seierstad, I., Steffensen, J.P., and Vinther, B. M.: A 60 000 year Greenland stratigraphic ice core chronology, Clim. Past, 4~~(1)~~, 47-57, https://doi.org/10.5194/cp-4-47-2008, 2008.

Talbot, M. R., and Johannessen, T.: A high resolution palaeoclimatic record for the last 27,500 years in tropical West Africa from the carbon and nitrogen isotopic composition of lacustrine organic matter, Earth Planet. Sci. Lett., 110~~(1-4)~~, 23-37, https://doi.org/10.1016/0012-821X(92)90036-U, 1992.

Tjallingii, R., Claussen, M., Stuut, J. B. W., Fohlmeister, J., Jahn, A., Bickert, T., Lamy, F., and Röhl, U.: Coherent high-and low-latitude control of the northwest African hydrological balance, Nat. Geosci., 1~~(10)~~, 670-675, https://doi.org/10.1038/ngeo289, 2008.

Trend-Staid, M., and Prell, W. L.: Sea surface temperature at the Last Glacial Maximum: A reconstruction using the modern analog technique. Paleoceanography, 17, 17-1, https://doi.org/10.1029/2000PA000506, 2002.

Van De Kamp, P. C.: Arkose, subarkose, quartz sand, and associated muds derived from felsic plutonic rocks in glacial to tropical humid climates, J. Sediment. Res., 80~~(10)~~, 895-918, https://doi.org/10.2110/jsr.2010.081, 2010.

Vriend, M., Groot, M. H. M., Hooghiemstra, H., Bogotá-Angel, R. G., and Berrio, J. C.: Changing depositional environments in the Colombian Fúquene Basin at submillennial time-scales during 284-27 ka from unmixed grain-size distributions and aquatic pollen, Neth J Geosci., 91~~(1-2)~~, 199-214, https://doi.org/10.1017/S0016774600001591, 2012.

Waelbroeck, C., Pichat, S., Böhm, E., Lougheed, B. C., Faranda, D., Vrac, M., Missiaen, L., Vazquez Riveiros, N., Burckel, P., Lippold, J., Arz, H.W., Dokken, T., and Dapoigny, A.: Relative timing of precipitation and ocean circulation changes in the western equatorial Atlantic over the last 45 kyr. Clim. Past, 14~~(9)~~, 1315–1330. https://doi.org/10.5194/cp-14-1315-2018, 2018.

Wang, C.: Variability of the Caribbean low-level jet and its relations to climate. Clim. Dyn, 29, 411-422, https://doi.org/10.1007/s00382-007-0243-z, 2007

Warken, S.F., Scholz, D., Spötl, C., Jochum, K.P., Pajón, J.M., Bahr, A., and Mangini, A.: Caribbean hydroclimate and vegetation history across the last glacial period. Quat Sci Rev, 218, 75-90, https://doi.org/10.1016/j.quascirev.2019.06.019, 2019.

Con formato: Color de fuente: Automático
Código de campo cambiado
Con formato: Color de fuente: Automático
Código de campo cambiado
Con formato: Color de fuente: Automático
Con formato: Inglés (Estados Unidos)
Con formato: Color de fuente: Automático
Con formato: Color de fuente: Automático
Código de campo cambiado
Código de campo cambiado
Con formato: Color de fuente: Automático
Con formato: Color de fuente: Automático
Código de campo cambiado
Con formato: Color de fuente: Automático
Con formato: Color de fuente: Automático
Código de campo cambiado
Con formato: Color de fuente: Automático
Con formato: Color de fuente: Automático
Código de campo cambiado
Con formato: Color de fuente: Automático
Con formato: Color de fuente: Automático
Código de campo cambiado
Con formato: Color de fuente: Automático
Con formato: Color de fuente: Automático
Código de campo cambiado
Con formato: Color de fuente: Automático
Con formato: Color de fuente: Automático
Código de campo cambiado
Con formato: Color de fuente: Automático

Warken, S. F., Vieten, R., Winter, A., Spötl, C., Miller, T. E., Jochum, K. P., Schröder-Ritzrau, A., Mangini, A., and Scholz, D.: Persistent link between Caribbean precipitation and Atlantic Ocean circulation during the Last Glacial revealed by a speleothem record from Puerto Rico, Paleoceanogr Paleoclimatol., 35~~(11)~~, https://doi.org/10.1029/2020PA003944, 2020

Weltje, G. J. (Ed.): Provenance and dispersal of sand-sized sediments: Reconstruction of dispersal patterns and sources of sand-sized sediments by means of inverse modelling techniques, Utrecht University, The Netherlands, 1994.

~~Weltje, G. J., and Tjallingii, R.: Calibration of XRF core scanners for quantitative geochemical logging of sediment cores: Theory and application, Earth Planet. Sci. Lett., 274(3-4), 423-438, https://doi.org/10.1016/j.epsl.2008.07.054, 2008.~~

Weltje, G., Bloemsma, M., Tjallingii, R., Heslop, D., Röhl, U., and Croudace, I.: Prediction of Geochemical Composition from XRF Core Scanner Data: A New Multivariate Approach Including Automatic Selection of Calibration Samples and Quantification of Uncertainties, in: Micro-XRF Studies of Sediment Core, edited by: Croudace, I., and Rothwell, R., Springer, Dordrecht, The Netherlands, https://doi.org/10.1007/978-94-017-9849-5_21, 2015.

Wersin, P., Höhener, P., Giovanoli, R., and Stumm, W.: Early diagenetic influences on iron transformations in a freshwater lake sediment. Chem. Geol., 90, 233–252., https://doi.org/10.1016/0009-2541(91)90102-W, 1991.

Whyte, F.S., Taylor, M.A., Stephenson, T.S., and Campbell, J.D.: Features of the Caribbean low level jet. Int J Climatol., 28, 119-128, https://doi.org/10.1002/joc.1510, 2008.

Yarincik, K. M., Murray, R. W., and Peterson, L. C.: Climatically sensitive eolian and hemipelagic deposition in the Cariaco Basin, Venezuela, over the past 578,000 years: Results from Al/Ti and K/Al, Paleoceanography, 15~~(2)~~, 210-228, https://doi.org/10.1029/1999PA900048, 2000.

Yu S.L., Hamrick J.M., and Lee D. (1984) Wind Effects on Air-Water Oxygen Transfer in a Lake. In: Gas Transfer at Water Surfaces. Water Science and Technology Library, vol 2, edited by: Brutsaert W., and Jirka G.H., Springer, Dordrecht. The Netherlands, https://doi.org/10.1007/978-94-017-1660-4_33, 1984

Zarriess, M., Johnstone, H., Prange, M., Steph, S., Groeneveld, J., Mulitza, S., and Mackensen, A.: Bipolar seesaw in the northeastern tropical Atlantic during Heinrich stadials. Geophys, Res. Lett., 38~~(4)~~, L04706, https://doi.org/10.1029/2010GL046070, 2011.

Ziegler, M., Nürnberg, D., Karas, C., Tiedemann, R., and Lourens, L. J.: Persistent summer expansion of the Atlantic Warm Pool during glacial abrupt cold events, Nat. Geosci., 1~~(9)~~, 601-605, https://doi.org/10.1038/ngeo277, 2008.

Con formato: Color de fuente: Automático
Con formato: Color de fuente: Automático
Código de campo cambiado
Código de campo cambiado
Con formato: Color de fuente: Automático
Con formato: Color de fuente: Automático
Código de campo cambiado
Código de campo cambiado
Con formato: Color de fuente: Automático
Con formato: Color de fuente: Automático
Código de campo cambiado
Con formato: Color de fuente: Automático
Código de campo cambiado
Con formato: Color de fuente: Automático
Con formato: Color de fuente: Automático
Código de campo cambiado
Con formato: Color de fuente: Automático
Con formato: Color de fuente: Automático
Código de campo cambiado
Con formato: Color de fuente: Automático
Con formato: Color de fuente: Automático